Power Electronic Systems
Laboratory

IEEE Transactions on Power Electronics, Vol. 28, No. 1, pp. 176-198, January 2013

The Essence of Three-Phase PFC Rectifier Systems - Part I

J. W. Kolar,
T. Friedli

Eidgenössische Technische Hochschule Zürich
Swiss Federal Institute of Technology Zurich

The Essence of Three-Phase PFC Rectifier Systems—Part I

Johann W. Kolar, *Fellow, IEEE*, and Thomas Friedli, *Member, IEEE*

***Abstract*—In the first part of this paper, three-phase power factor correction (PFC) rectifier topologies with sinusoidal input currents and controlled output voltage are derived from known single-phase PFC rectifier systems and/or passive three-phase diode rectifiers. The systems are classified into hybrid and fully active pulsewidth modulation boost-type or buck-type rectifiers, and their functionality and basic control concepts are briefly described. This facilitates the understanding of the operating principle of three-phase PFC rectifiers starting from single-phase systems, and organizes and completes the knowledge base with a new hybrid three-phase buck-type PFC rectifier topology denominated as SWISS Rectifier. Finally, core topics of future research on three-phase PFC rectifier systems are discussed, such as the analysis of novel hybrid buck-type PFC rectifier topologies, the direct input current control of buck-type systems, and the multi-objective optimization of PFC rectifier systems. The second part of this paper is dedicated to a comparative evaluation of four rectifier systems offering a high potential for industrial applications based on simple and demonstrative performance metrics concerning the semiconductor stresses, the loading and volume of the main passive components, the differential mode and common mode electromagnetic interference noise level, and ultimately the achievable converter efficiency and power density. The results are substantiated with selected examples of hardware prototypes that are optimized for efficiency and/or power density.**

***Index Terms*—AC–DC converter, boost, buck, overview, pulsewidth modulation (PWM) rectifier, PFC rectifier, power factor correction (PFC), rectifier, review, Swiss rectifier, three-phase.**

I. Introduction

THE POWER electronics supply of high-power electrical systems from the three-phase ac mains is usually carried out in two stages, i.e., the mains ac voltage is first converted into a dc voltage and then adapted to the load voltage level with a dc–dc converter with or without galvanic isolation (cf., Fig. 1). Often only one direction of power flow has to be provided; furthermore, coupling to the mains is typically implemented over only three conductors, i.e., without a neutral conductor.

In the simplest case, the rectification can be done by unidirectional three-phase diode rectifiers with capacitive smoothing of the output voltage and inductors on the ac or dc side (cf., Fig. 2). The low complexity and high robustness (no control, sensors, auxiliary supplies, or electromagnetic interference (EMI) filtering) of this concept must, however, be weighed against the disadvantages of relatively high effects on the mains and an unregulated output voltage directly dependent on the mains voltage level.

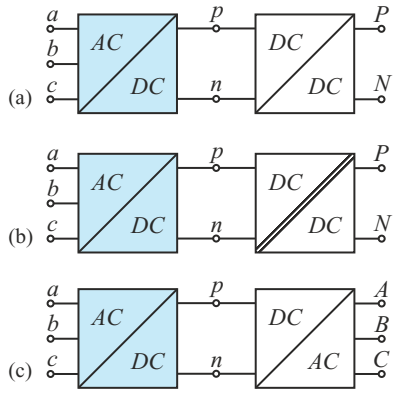

Fig. 1. Block diagrams of typical converter configurations for supplying electrical loads from the three-phase ac mains. (a) Three-phase ac–dc converter with nonisolated dc–dc converter (e.g., for the coupling of dc distribution systems to the three-phase mains or as a mains interface for high-power isolated loads, e.g., lighting systems). (b) Three-phase ac–dc converter with isolated dc–dc converter (e.g., for telecom power supplies, welders, or induction heating systems). (c) Three-phase ac–dc converter and three-phase dc–ac converter (inverter) without isolation (e.g., for variable speed drives).

The mains behavior of a power converter is characterized, in general, by the power factor λ, and/or the fundamental current-to-voltage displacement angle Φ, and the total harmonic distortion of the input current $\mathrm{THD_i}$ which are related by the equation

$$\lambda = \frac{1}{\sqrt{1+\mathrm{THD_i^2}}}\cos(\Phi)\ . \tag{1}$$

The conduction state of the passive rectifiers shown in Fig. 2(a) and (b) is essentially determined by the mains line-to-line voltages, whereby only two diodes carry current at the same time, except the commutation intervals. This means that each diode of the positive and negative bridge halves carries current only for one third of the mains period, i.e., for 120°. Hence, the phase currents for industrially applicable values of the smoothing inductance show 60°-wide intervals with zero current that result in a relatively high low-frequency harmonic content or a $\mathrm{THD_i} \approx 30\%$. In order to avoid voltage distortions resulting from voltage drops across the inner (inductive) mains impedance or the excitation of resonances in the distribution grid a $\mathrm{THD_i} < 5\%$ at rated power is often required. For aircraft on-board power supplies, relatively high inner mains impedances exist and thus even stricter limits, i.e., a $\mathrm{THD_i} < 3\%$

Manuscript received December 29, 2011; revised April 2, 2012; accepted April 18, 2012. Date of current version September 11, 2012. Recommended for publication by Associate Editor B. Lehman.

J. W. Kolar is with the Power Electronic Systems Laboratory, Swiss Federal Institute of Technology, Zurich 8092, Switzerland (e-mail: kolar@lem.ee.ethz.ch).

T. Friedli was with the Power Electronic Systems Laboratory, Swiss Federal Institute of Technology, Zurich 8092, Switzerland. He is now with ABB Switzerland Ltd., Turgi 5300, Switzerland (e-mail: thomas.friedli@ieee.org).

Color versions of one or more of the figures in this paper are available online at http://ieeexplore.ieee.org.

Digital Object Identifier 10.1109/TPEL.2012.2197867

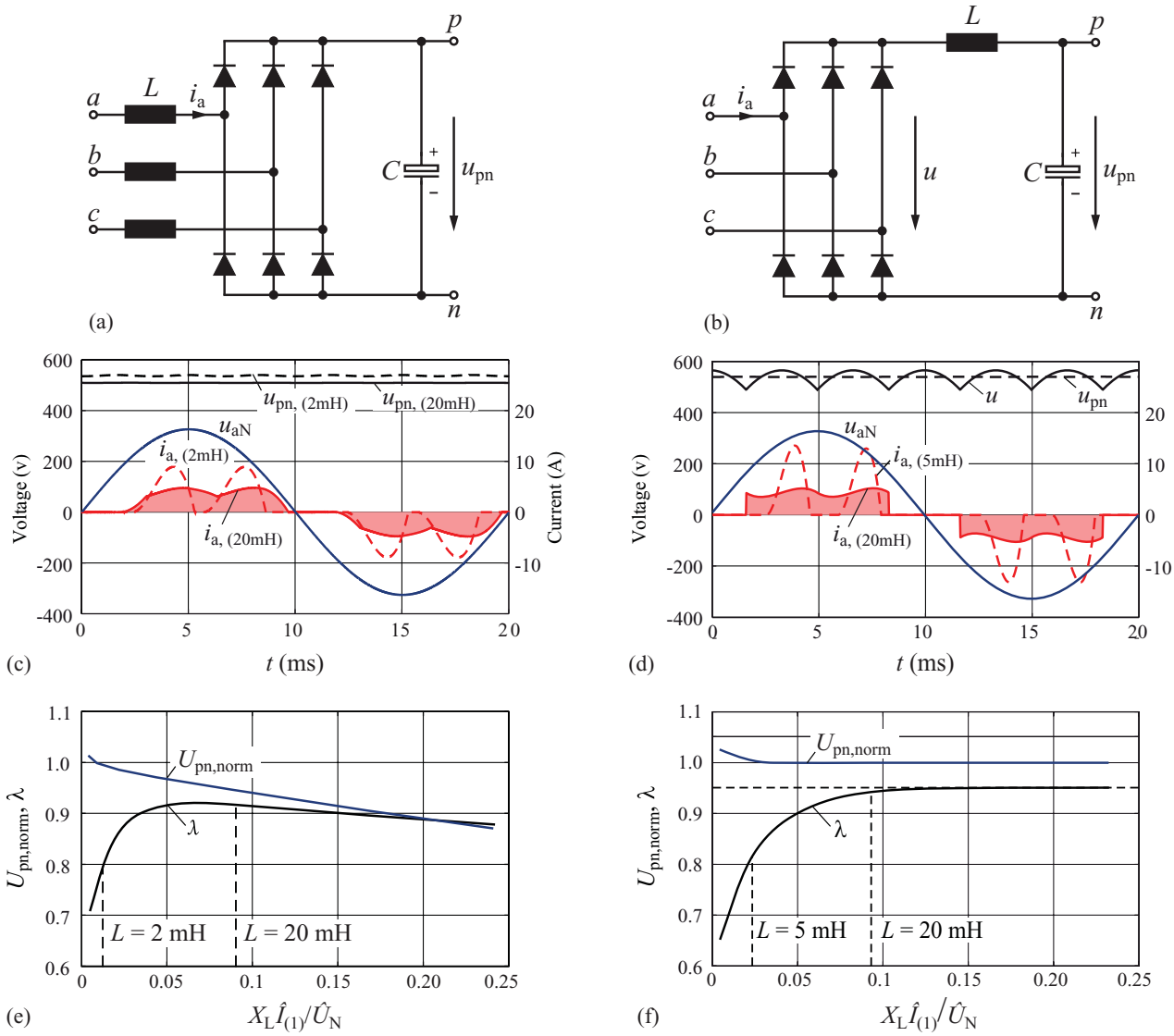

Fig. 2. Passive three-phase diode rectification. a) Smoothing inductors L on the ac side. (b) Smoothing inductor L on the dc side. (c) and (d) Corresponding input current waveforms. (e) and (f) Normalized global average value $U_{\mathrm{pn,norm}} = \pi/(3\sqrt{2}) \cdot U_{\mathrm{pn}}/U_{\mathrm{N,ll,rms}}$ of the global average output voltage U_{pn} and power factor λ at the input. (Simulation parameters: rms line-to-line voltage $U_{\mathrm{N,ll,rms}} = 400\,\mathrm{V}$, mains frequency $f_{\mathrm{N}} = 50\,\mathrm{Hz}$, smoothing capacitance on the dc side $C = 1\,\mathrm{mF}$, and smoothing inductance $L = [1\,\mathrm{mH} \ldots 45\,\mathrm{mH}]$ with $X_{\mathrm{L}} = 2\pi f_{\mathrm{N}} L$.)

(cf., DO160F, MIL-461F), have to be fulfilled. This mains current quality can be achieved only by means of active power factor correction (PFC) rectifier systems.

It should be noted that for three-phase systems, the generally used designation *PFC Rectifier* is partly misleading, since passive rectifiers, for industrially used values of the smoothing inductance $[X_{\mathrm{L}}\hat{I}_{(1)}/\hat{U}_{\mathrm{N}} = 0.05 \ldots 0.15$ according to Fig. 2(e) and (f)], already exhibit a high-power factor of $\lambda = 0.9 \ldots 0.95$ because of the low phase-shift of the power-forming mains current fundamental component and the associated phase voltage (cf., (1) for $\cos(\Phi) = 1$ and $\mathrm{THD_i} \approx 30\%$, [1], [2]). PFC rectifiers, hence, achieve with regard to the mains current (at rated operation) above all a reduction of the current harmonics but only a slight improvement in the power factor ($\lambda > 0.99$ at the rated operating point is typically targeted).

A further important aspect of the use of active (PFC) rectifier systems is the possibility to control the output dc voltage to a constant value, independent of the actual mains voltage (Europe: $U_{\mathrm{N,ll,rms}} = 400\,\mathrm{V}$; USA: $U_{\mathrm{N,ll,rms}} = 208\,\mathrm{V}$; Japan: $U_{\mathrm{N,ll,rms}} = 173\,\mathrm{V}$, $U_{\mathrm{N,ll,rms}}$ denominates the rms value of the mains line-to-line voltage). A converter stage on the output side (cf., Fig. 1) can, thus, be dimensioned to a narrow voltage range. The mains voltage range must be considered only for the dimensioning of the rectifier stage (the delivery of a given rated power, e.g., at half of the input voltage, leads to a doubling of the input current that must be mastered by the power semiconductors, passive power components and the EMI filter) or a relatively high and well-defined voltage level is available for the generation of the output (load) voltage [cf., Fig. 1(c)].

The requirements placed on active PFC rectifier systems can, thus, be summarized as follows:

1) sinusoidal input current according to regulations regarding the mains behavior of three-phase rectifier systems (EN 61000-3-2 if < 16 A, 61000-3-4 if > 16 A); in industry, however, typically independent of the concrete application, a $\mathrm{THD_i} < 5\%$ is required (at the rated operating point);
2) ohmic fundamental mains behavior ($\cos(\Phi) > 0.99$);
3) regulated output voltage; depending on the required level of the output dc voltage relative to the mains voltage, a system with boost-, buck-, or buck–boost-type characteristic has to be provided;
4) mastering of a mains phase failure, i.e., for interruption of one mains phase, continued operation at reduced power and unchanged sinusoidal current shape should be possible;
5) unidirectional power flow, perhaps with (limited) capability of reactive power compensation. Often, because of the supply of a purely passive load (e.g., telecom power supply), only unidirectional energy conversion has to be provided or as for aircraft on-board power supplies, no feedback of energy into the mains is permitted;
6) compliance with specifications regarding electromagnetic, especially conducted interference emissions by means of suitable EMI filtering.

The designation *three-phase PFC rectifier* chosen in this paper implies both sinusoidal mains current shaping and regulation of the dc output voltage. Here, it should be noted that an active harmonic filter [3] of lower rated power arranged in parallel to a passive rectifier system would also enable a sinusoidal mains current, but no regulation of the output voltage. Accordingly, because of the system-related advantage of a constant supply voltage of a load side converter, a PFC rectifier system is often preferred over active filtering despite the larger implementation effort, i.e., the conversion of the entire output power.

Parallel to the development of single-phase PFC rectifier circuits, numerous concepts for three-phase PFC rectifier systems have been proposed and analyzed over the last two decades. However, the topological relationships between the circuits and a comprehensive classification have received relatively little attention. Furthermore, the basic function of the circuits was typically treated by space vector calculation, analogous to three-phase drive systems, which is not immediately comprehensible on the basis of knowledge of dc power supply technology or single-phase PFC rectifier circuits.

The goal of the present work is, hence, to develop the concepts of three-phase PFC rectifiers, starting from known single-phase PFC rectifier systems, and to explain as clearly as possible their basic function and control, without reference to analysis techniques being specific to three-phase converter concepts. Details of the pulsewidth modulation (PWM) and a detailed mathematical analysis are omitted, i.e., only the operating range of the systems is clarified with regard to output voltage and mains current phase angle. Furthermore, the dimensioning of the power semiconductors, the main passive components, and the EMI filter is briefly discussed.

To keep matters short, the considerations remain limited to unidirectional, nonisolated systems and, here, to those circuits that come into question with regard to implementation effort for industrial applications or have already found such applications. Numerous theoretically interesting circuit proposals of high complexity and/or high-component loading are, hence, not considered. In particular, no circuits are discussed that fundamentally demand low-frequency passive components, e.g., dimensioned for sixfold mains frequency. Passive six- or twelve-pulse rectifier systems [5], hybrid rectifier circuits with passive third harmonic current injection networks [6], [7], direct single-stage (matrix-converter-based) rectifier systems [8], or soft-switching topologies [9], [10] are thus also not treated.

In the following, in Section II, a comprehensive classification of unidirectional three-phase rectifier systems is presented that for completeness also includes purely passive systems. For PFC rectifier circuits, a division is made between circuits that are fully active and hybrid, i.e., partially mains-commutated, and partially self-commutated systems. With regard to the basic structure, phase-modular and direct three-phase systems are distinguished and subsequently treated in more detail in Sections III and IV with reference to selected examples. Apart from systems with boost-type characteristic, buck-type PFC rectifier systems are also discussed, which were not considered in [11], but will be of special interest in future in connection with the charging of electric vehicle batteries or the supply of dc distribution grids. The ordering and complementation of the knowledge base of three-phase buck-type PFC rectifier systems leads to a new hybrid circuit concept (SWISS rectifier) that is characterized by low complexity of the power circuit and control, and thus of particular interest for industrial applications.

In part II of this paper [65], a comparative evaluation of four selected boost-type and buck-type PFC systems are presented, which is intended to provide an aid for the choice of suitable circuit concepts in industrial development projects. For this purpose, characteristic measures (performance indices) are identified that enable a holistic and demonstrative rectifier system comparison. The comparison is performed for latest generation insulated gate bipolar transistor (IGBT) devices and compared with a more advanced implementation using state-of-the-art SiC JFET power transistors. In the sense of support for the dimensioning of the circuits, the current stresses of the main circuit components are briefly summarized in the form of simple analytical expression, and the differential mode and common mode EMI filtering of the systems discussed.

II. CLASSIFICATION OF UNIDIRECTIONAL THREE-PHASE RECTIFIER SYSTEMS

In Fig. 3, a classification of unidirectional three-phase rectifier circuits is shown that for completeness also includes purely *passive systems* which:

1) contain no turn-off power semiconductors, i.e.;
2) work purely mains-commutated;
3) employ low frequency, i.e., passive components for output voltage smoothing and mains current shaping and, where applicable, mains or autotransformers for the phase-shift of several converter stages working in parallel or series (multipulse rectifier circuits).

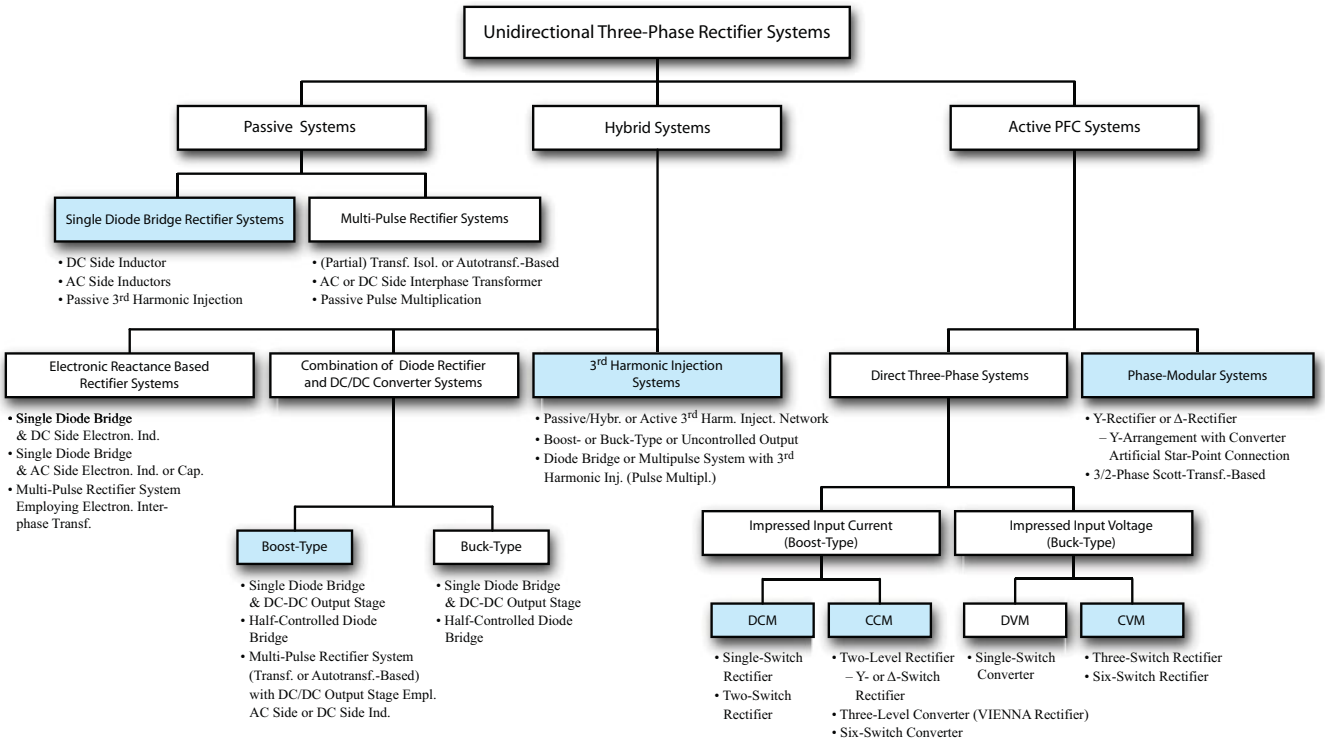

Fig. 3. Classification of (unidirectional) three-phase rectifier topologies into passive, hybrid, and active systems with boost- or buck-type characteristic. For each rectifier subgroup, references to publications are given in [4], in which the corresponding circuit concept was presented first or a detailed description is provided. The boxes of the converter groups, discussed in this paper, are highlighted by shading. For details of rectifier topologies not discussed in this paper, see [4].

Furthermore, since here only diode and not thyristor circuits are considered, there is no possibility of output voltage regulation.

An approximately sinusoidal mains current and/or partial elimination of low-frequency harmonics in the input current is, thus, only obtainable with multipulse systems, i.e., for 12-, 18-, or 36-pulse rectifier circuits. In industry, multipulse rectifiers, because of their low complexity and great robustness, are mainly used at high power (>100 kW) as mains interfaces, where the supply is typically direct from the medium voltage mains whose low inner impedance allows higher input current harmonics to be accepted.

The coupling and/or partial integration of a passive rectifier and of an active circuit part implemented with power semiconductors that can be actively switched OFF leads to *hybrid rectifier circuits*.

These systems fundamentally allow a regulation of the output voltage and a sinusoidal control of the mains current; however, a limitation to voltage regulation is possible (e.g., in the case of a diode bridge with downstream dc–dc converter) or to sinusoidal current shaping (active-filter-type third harmonic current injection, cf., Section IV or [12]–[17]). Furthermore, low-frequency filter components of passive rectifier systems may be replaced/emulated by high-frequency PWM converters of relatively low rated power (electronic inductor [18], [19]), e.g., in the sense of an increase of the power density. With an ac-side arrangement of these electronic reactances, via a change in the inductance or capacitance value in operation, a limited possibility of voltage regulation exists (magnetic energy recovery switch concept [20], [21]).

Third harmonic injection concepts form a major group of hybrid rectifier circuits. Here, current is injected by a passive or active injection network always into that phase which would not carry current in the case of conventional diode bridge rectification. The current waveforms of the two other phases are shaped in such a way that as a result, sinusoidal current flows in all phases. The rectifier function of these systems is implemented by a diode bridge on the input side. The active network for current shaping, injection, and voltage regulation, arranged on the dc side, may thus be considered essentially as a dc–dc converter working on a time-varying (six-pulse) dc input voltage. The circuits are, hence, relatively simple, i.e., may be analyzed without specific knowledge of three-phase converter systems and exhibit relatively low complexity, also regarding control. The essential characteristics of hybrid rectifier circuits may, thus, be summarized as follows:

1) mains-commutated (diode circuits) and forced-commutated, circuit sections implemented with power semiconductors that can be actively switched OFF;
2) low frequency and/or switching frequency passive components;
3) output voltage regulation and/or sinusoidal mains current shaping by turn-off power semiconductors.

In this study, only those hybrid rectifier circuits are considered which exhibit regulated output voltage and sinusoidal mains current, and exclusively switching frequency passive components.

Integration of turn-off power semiconductors into the bridge-legs of a passive system, finally, leads to *active PFC rectifier systems*. Essential features of these systems are:

1) forced commutation (only for systems with impressed output current partly natural commutations occur, depending on the position of the switching instant in the mains period);
2) exclusively switching frequency passive components;
3) regulated output voltage.

As described in more detail in Section IV, these systems exhibit, in general, bridge topologies and, here, bridge-legs of same structure, i.e., *phase symmetry*, and a similar configuration of the power semiconductors in the positive (connected to the positive output voltage bus) and negative bridge halves, i.e., *bridge symmetry*.

Apart from these direct three-phase versions (cf., Fig. 3), however, an implementation is also possible via a combination of single-phase PFC rectifier systems in star(Y)- or delta(Δ)-connection [cf., Fig. 5(a) and (b)]. These phase-modular versions, however, lead to three individual dc output voltages, i.e., a single output voltage can only be formed via isolated dc–dc converters that are connected to the rectifier outputs. An advantage of the phase-modular version is the possibility of realizing a three-phase system starting from existing already developed single-phase systems. However, it must be taken into account that with the star-connection a coupling of the phase system results. For the delta-connection, the high-input voltage of the modules has to be considered, which is defined by the mains line-to-line voltage and not by the phase voltage.

Apart from the topological distinction, a classification of the systems must also be carried out with regard to the available output voltage range, i.e., fundamentally into circuits with boost- or buck-type characteristic. As shown in Fig. 4, the lower or upper output voltage limits of the systems are defined by the mains line-to-line voltage. The voltage range, not covered by the two basic converter forms, is usually implemented in industry by means of a downstream dc–dc converter with boost- or buck-type characteristic. Alternatively, a three-phase extension of buck–boost [22], Cuk- or SEPIC-converters [23] could be used. Because of the high complexity of the resulting circuit, however, this approach is only of theoretical interest and is, hence, not described in more detail.

With regard to phase-modular rectifiers, it must be pointed out that buck-type converter systems enable a current shaping only in a part of the mains period [24]. Hence, for sinusoidal mains current, a boost function must be provided which results in a lower limit of the output voltages of the modules.

Note that systems with galvanic isolation of the output voltage are not treated in this paper. In many cases, isolation is achieved by a dc–dc output stage at high frequency, or is required directly at the supply of the systems for voltage adaptation, e.g., for connection to the medium voltage level. Alternatively, a transformer may be integrated directly into the rectifier structure. Such high-frequency isolated three-phase ac–dc matrix converter concepts [10], [25], [26], however, are characterized by a relatively high complexity of the power circuit and modulation and, hence, are of limited importance for industrial applications.

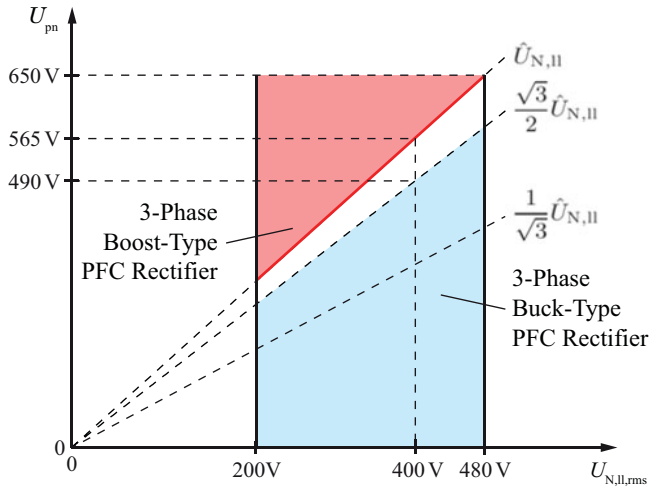

Fig. 4. Output voltage range of direct three-phase PFC rectifier systems with boost- or buck-type characteristic independent of the rms line-to-line mains voltage $U_{\mathrm{N,ll,rms}}$ (considered mains voltage range: $U_{\mathrm{N,ll,rms}} = 200\,\mathrm{V} \ldots 480\,\mathrm{V}$); $\hat{U}_{\mathrm{N,ll}}$ denominates the peak value of the line-to-line voltage. In addition, the lower output voltage limit of a single-phase boost-type PFC rectifier system ($U_{\mathrm{pn}} > 1/\sqrt{3}\,\hat{U}_{\mathrm{N,ll}}$), connected between a mains phase and the mains neutral, is shown.

III. Phase-Modular Rectifiers

Starting from the basic circuits of symmetrical three-phase loads, three-phase PFC rectifier systems can be implemented by star- or delta-connection of single-phase PFC rectifiers. The phase-modular systems, thus, formed will be termed in the following Y- or Δ-rectifiers according to the circuit structure. The phase modules, here, may exhibit a conventional topology or could be implemented as bridgeless, i.e., dual-boost converters, or ac-switch converters (cf., Fig. 10). They may contain an EMI filter or advantageously, a three-phase EMI filter could be installed common to all phase systems.

A. Y-Rectifier

Fig. 6 shows the circuit topology of a Y-rectifier with a bridgeless topology of the phase modules and an equivalent circuit of the ac-side system part. If the EMI filter is three-phase (not shown in Fig. 6) and the star-point N' is not connected to an artificial star-point, which could be formed, e.g., by filter capacitors, a switching frequency voltage $u_{\mathrm{N'N}}$ occurs between N' and the mains star-point N.

According to

$$\begin{aligned} L\frac{di_{\mathrm{a}}}{dt} &= u_{\mathrm{aN}} - (u_{\bar{\mathrm{a}}\mathrm{N'}} + u_{\mathrm{N'N}}) \\ L\frac{di_{\mathrm{b}}}{dt} &= u_{\mathrm{bN}} - (u_{\bar{\mathrm{b}}\mathrm{N'}} + u_{\mathrm{N'N}}) \\ L\frac{di_{\mathrm{c}}}{dt} &= u_{\mathrm{cN}} - (u_{\bar{\mathrm{c}}\mathrm{N'}} + u_{\mathrm{N'N}}) \end{aligned} \tag{2}$$

the impression of the ac currents is via the differences of the mains phase voltages and the voltages $u_{\bar{i}\mathrm{N'}}$ ($i = a, b, c$) formed at the input of the rectifier stages, so that the star-point voltage

$u_{\mathrm{N'N}}$ with consideration of

$$\frac{d}{dt}\left(i_{\mathrm{a}}+i_{\mathrm{b}}+i_{\mathrm{c}}\right)=0 \tag{3}$$

results in

$$u_{\mathrm{N'N}}=-\frac{1}{3}\left(u_{\bar{\mathrm{a}}\mathrm{N'}}+u_{\bar{\mathrm{b}}\mathrm{N'}}+u_{\bar{\mathrm{c}}\mathrm{N'}}\right)\ . \tag{4}$$

Therefore, with a free star-point N', a part of the rectifier input voltage $u_{\bar{i}\mathrm{N'}}$ advantageously does not form a current ripple, so that the values of the boost inductance may be reduced compared to a fixed star-point for the same ripple amplitude. This advantage is gained at the expense of a CM voltage $u_{\mathrm{N'N}}$ of the modules, which requires an appropriate CM filter.

As clearly shown by Fig. 6(b) and with regard to the fundamental of the input voltage required for the impression of the input current, the same conditions are present for the phase modules as for single-phase PFC rectifiers supplied from a mains phase. Therefore, despite the high-peak value of the line-to-line voltage of the European low-voltage grid ($\hat{U}_{\mathrm{N,ll}}=565\,\mathrm{V}$ and/or $U_{\mathrm{N,ll,rms}}=400\,\mathrm{V}$), the output voltage of the phase modules can be selected, e.g., at $U_{\mathrm{pn},i}=400\,\mathrm{V}$ and/or the power transistors may be implemented with 600-V superjunction power MOSFETs.

With regard to the fundamental input current, the system, thus, behaves as a symmetrical ohmic load with resistances $R=1/G^*$ in star-connection. Accordingly, for asymmetrical mains, there occurs in a phase with lower voltage a lower current amplitude, or a reduced supply of power to the respective output. This must be considered for setting the reference value of a downstream dc–dc converter.

Because of the phase-modular structure, three output voltages are to be regulated. Therefore, the voltage control is split into two parts. On the one hand, the power drawn from the mains, i.e., G^* is defined from the average control error of the three output voltages $u_{\mathrm{pn},i}$. On the other hand, a balancing of the output voltages is implemented, whereby in each case only the phase with the highest positive and the highest negative voltage value is taken into account [27], [30], [31]. As shown in Fig. 7, only for these phases, e.g., a and c, a higher instantaneous output power flow is present and, hence, the possibility of changing the output voltage value. Dependent on the difference between $U_{\mathrm{pn,a}}$ and $U_{\mathrm{pn,c}}$, an offset of the reference phase current values i_0^* is formed which, however, cannot be set by the phase current controllers because the free star-point N', $i_{\mathrm{a}}+i_{\mathrm{b}}+i_{\mathrm{c}}=0$ is unalterable. The phase currents, thus, keep their sinusoidal shape and the symmetry to the time axis. However, as could be shown by a more detailed analysis, for $i_0^*>0$, the switching state (100) is mainly used instead of (011) for the formation of the voltages $u_{\bar{\mathrm{i}}\mathrm{N'}}$ required for current impression. Similarly, for $i_0^*<0$ increasingly (011) is employed instead of (100). Both switching states are redundant with respect to the voltage formation and result in equal voltages $u_{\bar{\mathrm{a}}\bar{\mathrm{b}}}$, $\bar{u}_{\bar{\mathrm{b}}\bar{\mathrm{c}}}$, $u_{\bar{\mathrm{c}}\bar{\mathrm{a}}}$. However, for (100), primarily the output capacitor C_{c} is charged, and for (011) the capacitor C_{a} and thus an equalization of $U_{\mathrm{pn,a}}$ and $U_{\mathrm{pn,c}}$ is enabled. For (100), power also flows to output $u_{\mathrm{pn,b}}$, but because of the low instantaneous value of i_{b} in $\varphi_{\mathrm{N}}=\omega_{\mathrm{N}}t=(0^\circ,60^\circ)$ and/or the associated low output current, the output voltage $u_{\mathrm{pn,b}}$ is not significantly changed [31].

In connection with the balancing of the output voltages, it should be pointed out that a symmetrical mains current system can also be surprisingly maintained for unequal distribution of the input power to the three outputs, i.e., is also possible for asymmetrically loaded outputs.

To summarize, the total power drawn from the three-phase mains is set by G^* and the distribution of the power to the phases is determined by i_0^*. Shifting the power between always only two phases has the advantage that the fulfillment of $i_{\mathrm{a}}+i_{\mathrm{b}}+i_{\mathrm{c}}=0$ does not need to be specially observed since the third phase can always carry a resulting current. This procedure thus exhibits, compared to alternative concepts [29], a greater stability range and a significantly lower parameter sensitivity or greater robustness.

It should be emphasized that the balancing procedures described may be employed only in the case of a common EMI filter for all phases and/or for a free star-point N, which allows a variation of $u_{\mathrm{N'N}}$ with switching frequency. Here, the balancing of the output capacitor voltages and not a vanishing (low frequency) voltage difference of N' from the mains star-point N is of importance.

For employing individual EMI filters per module, on the other hand, only low-frequency potential changes in N' can occur and the balancing of the phase units can be with reference to the star-point voltage [33]. Alternatively, and/or in addition to balancing, N' can also be connected to an artificial star-point that is formed by a transformer circuit of low zero-sequence impedance and can be loaded with a zero-sequence current component occurring in the case of asymmetry [34], [35]. The disadvantage of this concept, basically known from the star-point formation in electrical networks, however, lies in the requirement of an additional inductive component of relatively large volume and weight.

In Fig. 8(a), the demonstrator of a highly compact version of a single-phase bridgeless PFC rectifier system [cf., Fig. 10(b)] is shown; Fig. 8(b) shows a highly efficient version of the same rectifier topology. Starting from these systems, Y-rectifiers with power densities of up to $5\ \mathrm{kW/dm^3}$ or efficiencies of $\eta>99\%$ may be implemented.

B. Δ-Rectifier

For delta-connection of the PFC rectifier modules [cf., Fig. 5(b)], the subsystems are decoupled, in contrast to the star-connection (Y-rectifier). The control can, therefore, be carried out, individually for each subsystem, in the same way as for single-phase PFC rectifiers. Balancing of the modules with respect to power consumption is of advantage in the sense of symmetrical loading of the mains, but is not absolutely necessary. However, the line-to-line voltage of the mains appears at the input to the modules. Hence, a relatively high-output voltage $U_{\mathrm{pn},i}>\sqrt{2}\,U_{\mathrm{N,ll,rms}}$ (typ. $U_{\mathrm{pn},i}=700\,\mathrm{V}\ldots800\,\mathrm{V}$ for the European low-voltage mains, taking into account voltage tolerances) or a high-blocking capability of the power semiconductors has to be provided. Alternatively, the

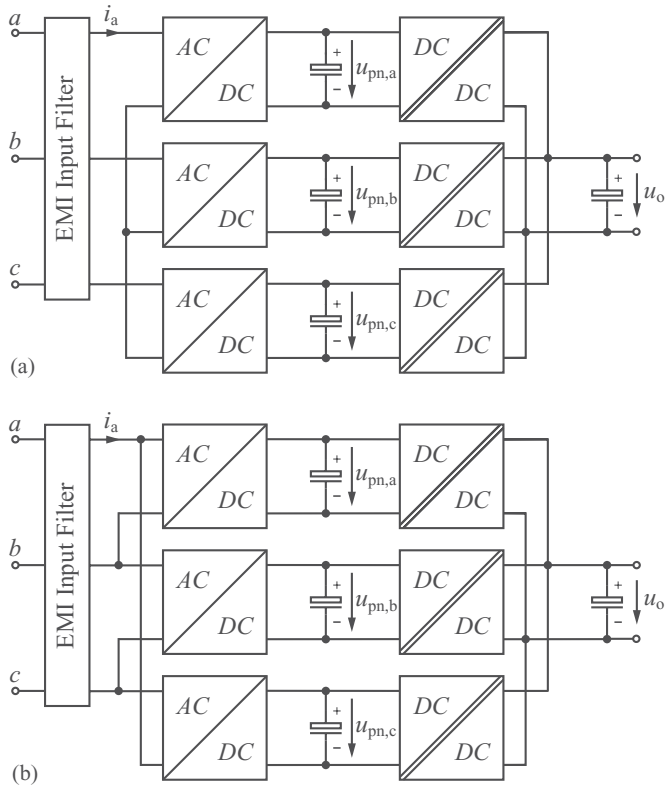

Fig. 5. Block diagram of phase-modular PFC rectifier systems [27]–[29]. (a) Star(Y)-connection / Y-rectifier and (b) delta(Δ)-connection / Δ-rectifier with output side isolated dc–dc converters. Instead of a common EMI input filter for all phases as used for (a) and (b), in terms of full modularity, also separate EMI filters could be implemented for each rectifier module.

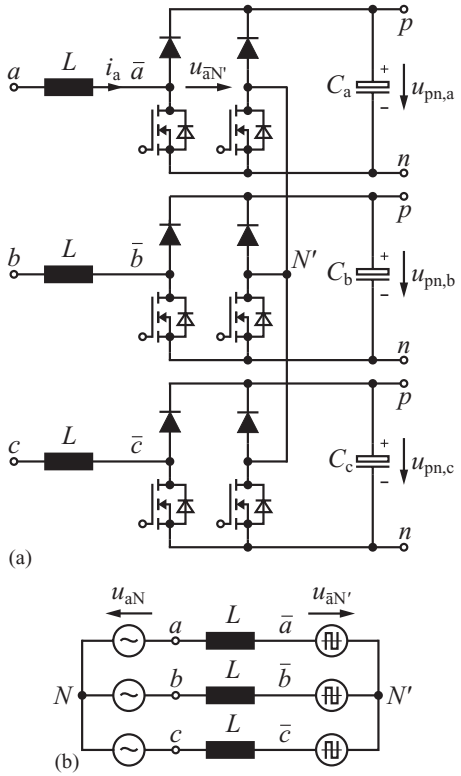

Fig. 6. (a) Basic structure of the Y-rectifier. (b) Equivalent circuit of the ac system part without the EMI input filter.

semiconductor-blocking voltage stress could be halved by means of a three-level topology. Also, a buck converter could be placed in front of each boost converter stage, i.e., in each phase, a buck–boost converter with a common inductor could be implemented. This would allow the output voltage level of the individual modules to be chosen similar as for the Y-rectifier with 400 V [36]. Then, only the transistors of the buck stage have to be designed for line-to-line voltages. However, an additional power transistor then lies in the current path, which leads to higher conduction losses.

At the input of the rectifier stages of the Δ-rectifier modules, for a two-level implementation of the boost output stages, voltages

$$u_{\bar{i}\bar{j}} = s_{ij}\text{sign}\,(i_{ij}) \in (0, +U_{\text{pn},i}, -U_{\text{pn},i}) \tag{5}$$

(s_{ij} designates the switching state of the power transistors S_{ij}; $i, j = \{a, b, c\}$) are formed that, apart from the switching state $s_{\text{ab}} = s_{\text{bc}} = s_{\text{ca}} = 0$, contain a switching frequency zero sequence voltage component u_0

$$\begin{aligned} u_{\bar{\text{a}}\text{b}} &= u'_{\bar{\text{a}}\text{b}} + u_0 \\ u_{\bar{\text{b}}\text{c}} &= u'_{\bar{\text{b}}\text{c}} + u_0 \\ u_{\bar{\text{c}}\text{a}} &= u'_{\bar{\text{c}}\text{a}} + u_0\ . \end{aligned} \tag{6}$$

As can be immediately seen via a delta–star transformation for the formation of the phase currents i_i, only the voltages $u'_{\bar{\text{a}}\text{b}}$,

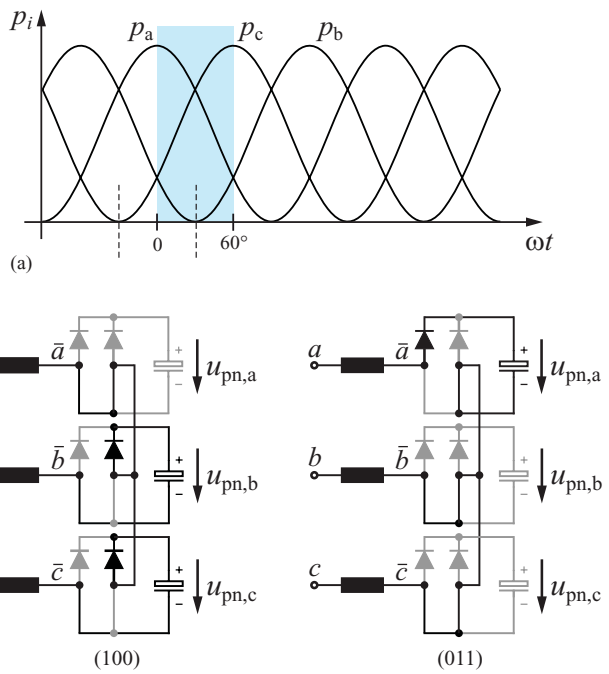

Fig. 7. (a) Time behavior of the instantaneous fundamental power of the phases of a Y-rectifier. (b) Redundant switching states concerning the resulting variation of the phase currents for $i_a > 0$, $i_b < 0$, $i_c < 0$ [valid within $\varphi_N = (-30°, +30°)$], which can be used for balancing the dc output voltages $u_{pn,a}$, $u_{pn,b}$, $u_{pn,c}$ of the phase modules.

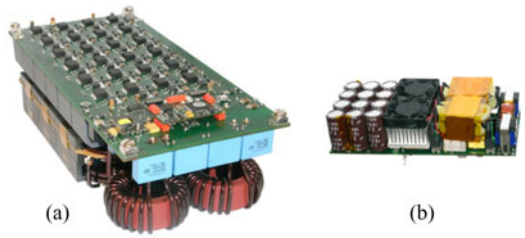

Fig. 8. Hardware demonstrator of (a) an ultra-efficient Y-rectifier phase module (nominal efficiency: $\eta_{\mathrm{nom}} > 99\%$, dimensions: 275 mm × 130 mm × 85 mm, power density: $\rho > 1.1\,\mathrm{kW/dm^3} = 18\,\mathrm{W/in^3}$) and (b) of an ultra-compact Y-rectifier phase module (dimensions: 175 mm × 80 mm × 42 mm, power density: $\rho > 5\,\mathrm{kW/dm^3} = 82\,\mathrm{W/in^3}$). The nominal output power of both systems is 3.3 kW [32].

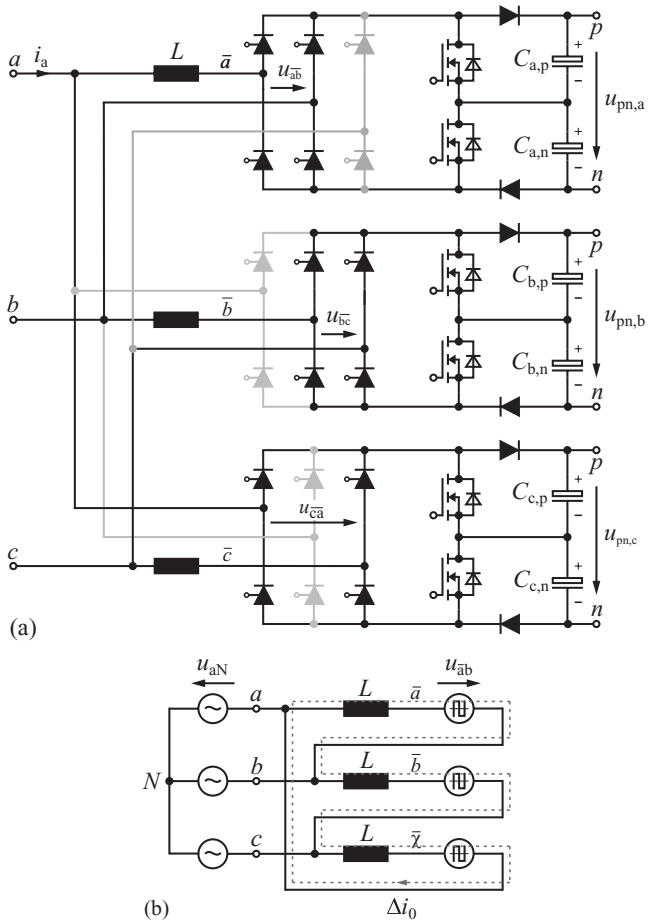

Fig. 9. (a) Basic structure of the Δ-rectifier, with thyristor bridges at the input of the modules to provide the nominal output power in the case of phase loss; three-level boost stages are employed to reduce the voltage stress of the power semiconductors. (b) Simplified ac-side equivalent circuit with the zero-sequence component Δi_0 of the input current ripples of the modules.

$u'_{\bar{b}c}$, $u'_{\bar{c}a}$, and/or the equivalent star-point phase voltages

$$u'_{\bar{a}N} = \frac{1}{3}\left(u'_{\bar{a}b} - u'_{\bar{c}a}\right)$$
$$u'_{\bar{b}N} = \frac{1}{3}\left(u'_{\bar{b}c} - u'_{\bar{a}b}\right)$$
$$u'_{\bar{c}N} = \frac{1}{3}\left(u'_{\bar{c}a} - u'_{\bar{b}c}\right) \tag{7}$$

with

$$u'_{\bar{a}b} + u'_{\bar{b}c} + u'_{\bar{c}a} = 0 \tag{8}$$

are effective. The zero-sequence voltage component

$$u_0 = \frac{1}{3}\left(u_{\bar{a}b} + u_{\bar{b}c} + u_{\bar{c}a}\right) \tag{9}$$

thus drives only a switching-frequency current within the delta-circuit. This means that for a three-phase EMI filter, the modulation is best designed through suitable synchronization of the carrier signals of the modules such that u_0 is maximized or a maximum fraction Δi_0 of the switching-frequency input current ripple of the modules is held within the delta circuit [29], [37]. There then results a minimum ripple of the phase currents i_i, and the EMI filter effort is minimized. However, this advantage should be weighed against full modularity/independence of the subsystems (also regarding switching and modulation), that is obtainable only with the configuration of an individual EMI filter per module.

An essential advantage of the Δ-rectifier is the availability of the full-rated power even for a failure of one mains phase. For this purpose, the modules must be connected as in Fig. 9(a) via three-phase thyristor bridges to the mains, and the thyristor bridges, on interruption of a mains phase, are switched over to the two remaining phases (cf., [29], [36]). However, this concept is applicable only for a suitably high-loading capacity of the remaining mains phases.

C. Discussion

Phase-modular systems allow the knowledge on single-phase PFC rectifier systems to be exploited relatively directly and/or allow for the development of a three-phase PFC rectifier system with low effort. However, this advantage can be realized only with a fully modular structure, i.e., with the arrangement of an individual EMI filter per module, so that the modulation methods for the reduction of ripple in the phase currents described earlier cannot be used. However, in any case, a balancing of the modules is required to assure a symmetrical loading of the mains. Here, the additional effort for measurement and signal processing required for the Y-rectifier should be noted.

Basically, due to the modular structure, three individual dc output voltages are formed that only with the aid of downstream isolated dc–dc converters can be employed for the supply of a single load. Furthermore, each module requires filtering of the power flow, which pulsates with twice the mains frequency, i.e., electrolytic capacitors of suitably high capacitance must be provided on the output side. On the other hand, the assurance of a mains-holdup to master the failure of a mains voltage half-cycle anyway requires a relatively high-output capacitance. Furthermore, by division of the overall system into three subsystems, a compact construction is supported and the cooling of the power components is simplified.

The essential advantage of the Y-rectifier is the lower voltage stress of the power semiconductors or the relatively low level of the output dc voltages. However, a direct coupling of the phase

modules is present, which especially for mastering of a phase failure requires a close coordination of the modules and, finally, a control circuit for the overall system. Hence, the advantage of modularity cannot be used for the control. Industrially, the system will, thus, probably remain of minor importance. In contrast, the modules of the Δ-rectifier work in a decoupled manner, and via a relatively simple expansion of the circuit topology, the full-rated power is available on phase failure. The disadvantage of the relatively high-output voltage and/or required blocking voltage capability of the power semiconductors in the modules ought to be alleviated in future by the availability of 1200-V SiC power JFETs or SiC power MOSFETs. Then also an additional buck converter stage could be implemented for each module, which enables to maintain the output voltage level given by single-phase PFC systems and therewith the use of already developed dc–dc converter circuits. On the whole, then, an excellent potential for industrial application of this system can be discerned.

IV. Direct Three-Phase PWM Rectifier Topologies

In the following, the topologies of important direct three-phase boost- and buck-type rectifier systems will be derived and briefly described with regard to their basic function and control. Boost systems will be developed by three-phase extension of known single-phase boost-type PFC circuits (cf., Fig. 10 and/or Fig. 26 in [32]); the circuit structures of the buck-type systems follow by extension of passive three-phase diode rectifiers with turn-off power semiconductors.

In general, the definition of three-phase converter topologies, should be under consideration of a high level of symmetry of the resulting circuit structure. Because of the identical nature of the phases of the supplying mains (pure ac voltages of same shape and amplitude), it is obvious to provide the same structure for the circuit branches connected to the phase terminals (phase symmetry). On the other hand, the symmetry of the positive and negative half-cycles of the ac input phase currents to be impressed by the rectifier system naturally leads to an identical arrangement of power semiconductors in the positive and the negative half of the phase-legs. In connection with the dc voltage to be formed, corresponding topologically to a positive and a negative output terminal, there, thus, results a three-phase bridge topology with symmetrical positive and negative bridge halves (bridge symmetry). For a dc–dc converter, connected to the rectifier output, this symmetry does not necessarily need to be maintained. Here, a decision could be made, e.g., by analysis and comparison of the CM EMI emissions and the conduction losses of a symmetrical or asymmetrical topology.

It should be noted that rectifier systems which violate one or both symmetry requirements, e.g., with the aim of reducing the implementation effort, can also enable the impression of mains ac currents and the formation of a regulated output dc voltage. However, a sinusoidal shape of the phase currents is possibly not feasible (cf., Section IV-A2 for systems showing phase symmetry but no bridge symmetry), and/or the output voltage or the modulation range of the circuits is limited compared to symmetric structures. Furthermore, in general, a more

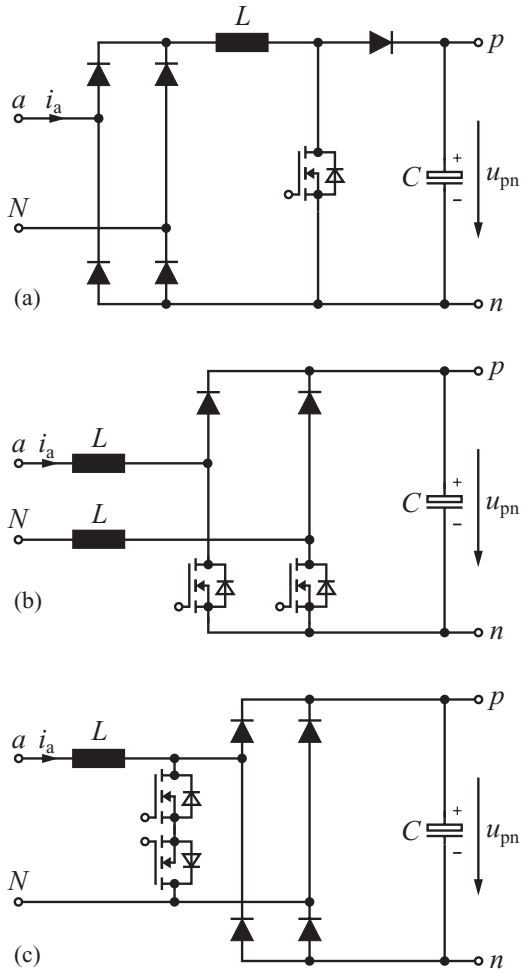

Fig. 10. Single-phase boost-type PFC rectifier systems; the three-phase extensions of the circuits leads to direct three-phase hybrid or active PFC rectifier systems with boost-type characteristic. (a) Conventional PFC rectifier, (b) bridgeless (dual-boost) PFC rectifier, and (c) PFC rectifier with ac-switch.

complex modulation results (cf., e.g., [38] as an example of a system with bridge symmetry but no phase symmetry). In addition, with missing phase or bridge symmetry, differing loadings of the individual power semiconductors occur. Asymmetrical circuits are, hence, treated within the scope of this work only as an intermediate step in the derivation of symmetrical circuits.

In the following, for all circuits, i.e., also for systems employing power semiconductors with high-blocking voltage stress (defined by the mains line-to-line voltage), power MOSFETs are shown as switching elements. This should point out the generally existing requirement of high-switching frequency or high-power density. An implementation of the power semiconductors would be possible with Si super-junction MOSFETs with a blocking voltage of 900 V [39] or in future with SiC JFETs (in a cascode configuration, [40]–[42]) or SiC MOSFETs [43]). Alternatively, 1200-V IGBTs, possibly with SiC freewheeling diodes could also be employed, however, with considerably lower switching frequency, due to the relatively high switch-off losses.

A. Boost-Type Systems

A three-phase extension of the conventional single-phase boost-type PFC rectifier [cf., Fig. 10(a)], i.e., the addition of a third bridge-leg to the input rectifier bridge, results in a hybrid rectifier structure shown in Fig. 11(a). The system enables a control of the output voltage, but the input current exhibits the characteristic block shape of passive-diode rectification with $\mathrm{THD_i} \approx 30\%$ [cf., Fig. 11(b)].

If the boost inductance is moved to the ac side and distributed over the phases [cf., Fig. 11(c)] and the mode of operation is changed to DCM at constant duty cycle of the power transistors, the switching frequency peak values of the discontinuous phase currents follow a sinusoidal envelope. However, as shown by more detailed analysis, low-frequency harmonics of the phase currents continue to occur [44]. A modulation of the transistor switch-on time with sixfold mains frequency [45], [46] and/or operation in boundary conduction mode also cannot completely eliminate the low-frequency current distortion, since the smallest phase current in each case always reaches zero prior to the other two phase currents and, thus, exhibits a zero current interval at switching frequency [44]. Accordingly, a relatively high-current quality is only attainable for high-voltage transfer ratios and/or a relatively short demagnetization time of the inductors L compared to the transistor switch-on time, i.e., for output voltages $U_{\mathrm{pn}} > 1\,\mathrm{kV}$ when operating in the European low-voltage mains. Because of this limitation, and the high peak current loading of the power semiconductors and the large EMI filter effort, this circuit concept has not been successful in industry.

Fundamentally, it should also be noted, here, that for three-phase converter systems, because of the relatively high power, operation in CCM is clearly preferable. Accordingly, the phase-shifted operation of several DCM converter stages, which would be possible for the system shown in Fig. 11(c), [47], [48], and is frequently used for single-phase systems (for power levels up to typ. 1 kW) is of minor importance.

1) Hybrid Third Harmonic Current Injection PFC Rectifier: An improvement in the input current quality of the circuit in Fig. 11(a) is only possible by extension of the controllability, i.e., by addition of a further power transistor (cf., Fig. 12). The currents in the positive and negative dc buses, i_+ and i_-, can then be controlled independently and proportional to the two phase voltages involved in each case in the formation of the output voltage of the diode bridge. If the difference of i_+ and i_- is then fed back via a current injection network (three four-quadrant switches, of which in each case only one is switched ON) into the mains phase which would not carry current for simple diode rectification, a sinusoidal current shape can be assured for all mains phases as shown below [49].

Because of the symmetries of the supplying mains voltage system, the mathematical proof of the sinusoidal current shaping can be limited to a 60°-wide interval of the mains period with, e.g., $u_{\mathrm{aN}} > u_{\mathrm{bN}} > u_{\mathrm{cN}}$, for which the injection switch S_{bYb} (in general, the injection switch of the phase with the smallest absolute voltage value) is continuously switched ON.

By suitable modulation of S_+, a current proportional to the mains phase voltage u_{aN} can then be impressed in L_+ or in the conducting diode $D_{\mathrm{a}+}$

$$i_+ = i_{\mathrm{a}} \tag{10}$$

whereby for the local average, i.e., the fundamental frequency component

$$\bar{i}_{\mathrm{a}} = G^* u_{\mathrm{aN}} \tag{11}$$

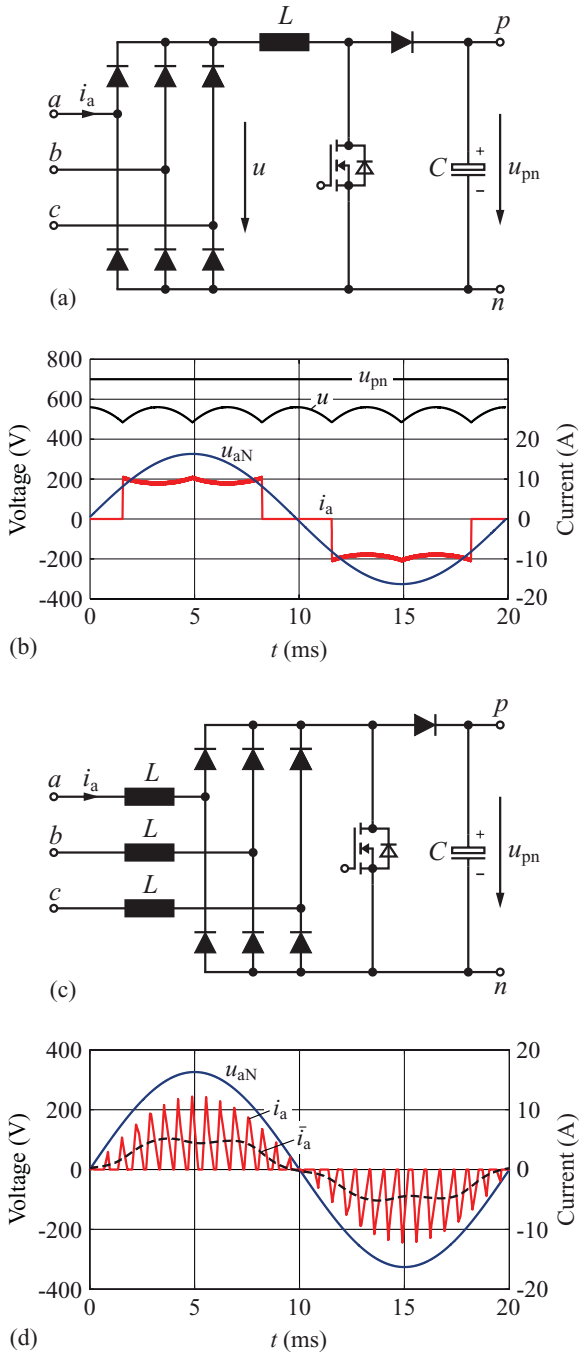

Fig. 11. Three-phase extension of the single-phase system shown in Fig. 10(a). (a) System structure and (b) corresponding mains voltage and mains current if the dc–dc boost converter stage operates in continuous conduction mode (CCM). (c) System structure if the boost inductor is shifted to the ac side and divided over the phases. (d) Corresponding mains voltage and current ($\bar{i}_{\mathrm{a}}$ refers to the local average value of the phase current i_{a}) for operation of the system in discontinuous conduction mode (DCM).

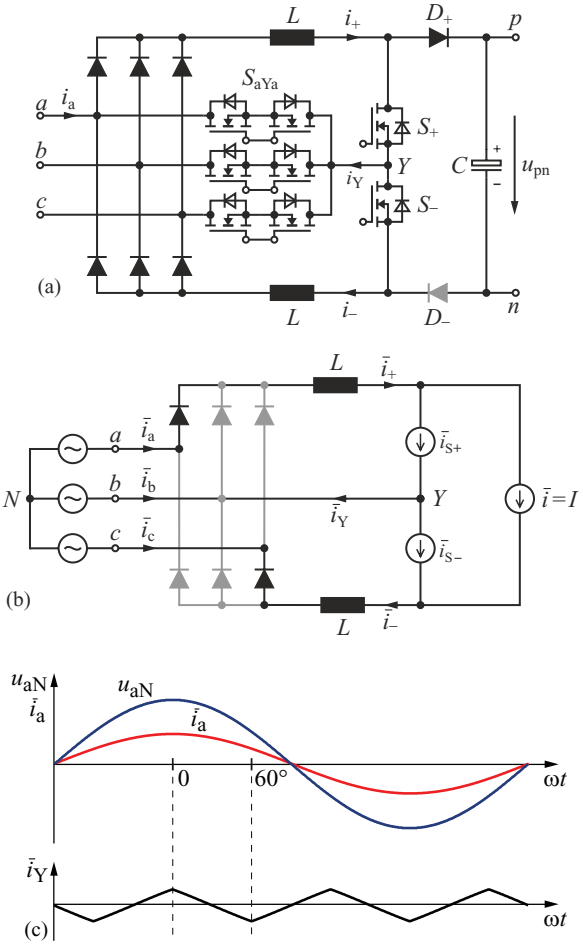

Fig. 12. (a) Basic structure of the hybrid third harmonic current injection rectifier [49]. (b) Local average equivalent circuit of the active system part for $u_{aN} > u_{bN} > u_{cN}$. (c) Waveforms of the phase voltage u_{aN}, the corresponding phase current i_a, and the injected current $\bar{i}_Y$. It would be advantageous to add a second freewheeling diode D_- in the negative bus to minimize the switching frequency CM voltage variation of the output. However, this would result in increased conduction losses.

has to apply. Correspondingly, by suitable modulation of S_-, a current

$$-i_- = i_C \tag{12}$$

proportional to u_{cN} can be impressed in L_- or D_{c-} with

$$\bar{i}_c = G^* u_{cN} \ . \tag{13}$$

The fundamental frequency conductance G^*, determining the rectifier input and/or power, is thereby defined by the output voltage controller. The switching of S_+ and S_- must not be carried out in a coordinated manner since freewheeling of i_+ and/or i_- is always possible via the freewheeling diodes D_+ and D_- or the diodes antiparallel to S_+ and S_- and the injection switch S_{bYb}.

For the injection current i_Y followed by Kirchhoffs' current law $i_+ - i_- - i_Y = 0$ or $i_a + i_c - i_Y = 0$, and on consideration of $i_b = -i_Y$ (injection switch S_{bYb} is switched ON)

$$i_b = -(i_a + i_c) \quad \text{and} \quad \bar{i}_b = -(\bar{i}_a + \bar{i}_c) \, . \tag{14}$$

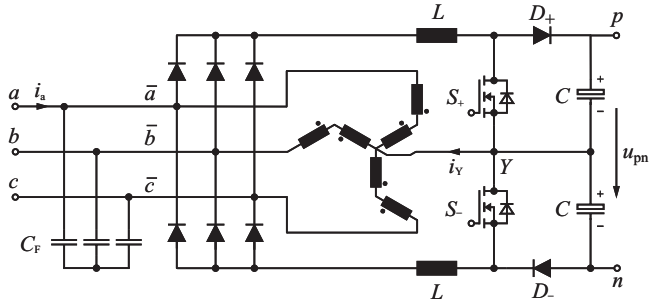

Fig. 13. Basic structure of the MINNESOTA rectifier with passive third harmonic current injection transformer network.

With (11), (12) and $u_{a0} + u_{b0} + u_{c0} = 0$ (symmetrical sinusoidal mains phase voltages) there then results

$$\bar{i}_b = -G^* (u_{aN} + u_{cN}) = G^* u_{bN} \ . \tag{15}$$

Accordingly, for all phases, a current shape proportional to the corresponding mains phase voltage is achieved. (Equation (14) could also be stated directly with reference to the current sum $i_a + i_b + i_c = 0$ forced to zero because of the free mains star-point *N*, but was derived here starting from the dc side in order to illustrate the function of the current injection.)

As would be clear from an analysis of further 60° sections of the mains period, the injection current i_Y exhibits threefold mains frequency. Thus, and in the sense of the classification chosen here, the rectifier system should be called *hybrid third harmonic current injection PFC rectifier*.

The feedback and/or injection of current occurs in Fig. 12 always into only one phase, which is selected by proper gating of the four-quadrant injection switches. Alternatively, the current injection could also be carried out by means of a purely passive injection network, e.g., a resonance network or a transformer circuit with low zero-sequence impedance (cf., MINNESOTA rectifier, [50]) shown in Fig. 13. However, it can then not be chosen in which phase a current is injected, but the feedback current can only be divided up into equal parts that are then injected into the phases. As shown in [4], a sinusoidal phase current waveform proportional to the mains voltage can also be attained therewith. However, the passive injection network shows a relatively large volume and weight. Furthermore, in comparison to the circuit in Fig. 12(a), a threefold amplitude of the injection current is required, so that the semiconductors of the converter stages that impress the currents i_+ and i_- must be dimensioned for a significantly higher current loading. Hence, considering the high-power density often demanded in industry, an active current injection is clearly preferable.

With regard to the operating range of the system, it must be stated that the output voltage must be selected significantly higher than the peak value of the line-to-line mains voltage, i.e., as $U_{pn} > \sqrt{6}\, U_{N,ll,rms}$ (as given in [51, Section II-D, p. 595]). As shown earlier, ohmic fundamental mains behavior can be attained, but no phase displacement of the mains current relative to the mains voltage is possible. However, it has to be emphasized that the system allows a continuation of operation with sinusoidal current shape (at reduced power) on failure of

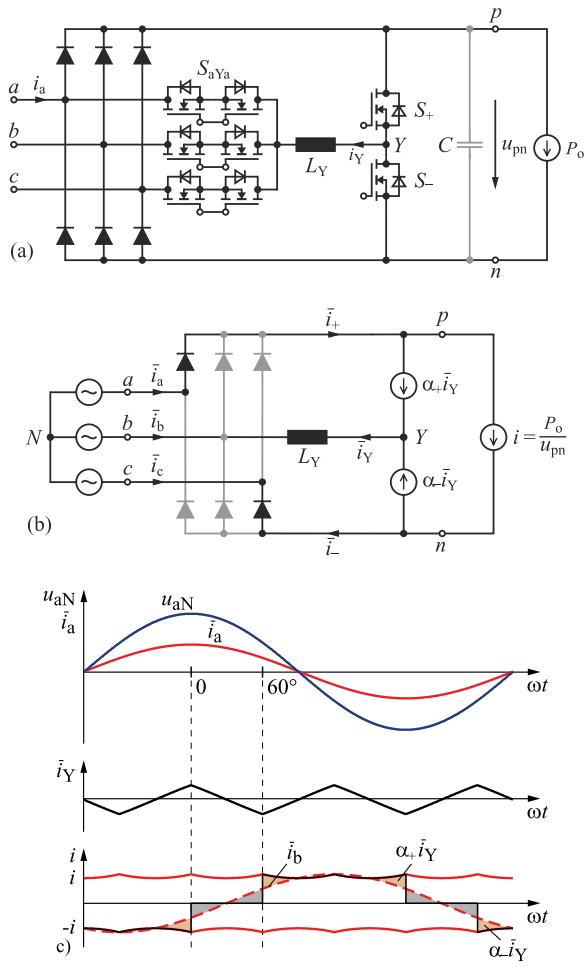

Fig. 14. (a) Hybrid third harmonic current injection active filter rectifier according to [4], [17]. (b) Local average equivalent circuit of the active part of the system for $u_{\mathrm{aN}} > u_{\mathrm{bN}} > u_{\mathrm{cN}}$. (c) Waveform of the phase voltage u_{aN}, the phase current $\bar{i}_{\mathrm{a}}$, the injection current $\bar{i}_{\mathrm{Y}}$, and the load current $i = P_{\mathrm{o}}/u_{\mathrm{pn}}$ at a constant output power P_{o}.

a mains phase. All injection switches then have to be blocked and a simultaneous gating of S_+ and S_- provided, so that the same conditions exist as for a single-phase PFC rectifier system operating on a mains line-to-line voltage.

2) Hybrid Third Harmonic Current Injection Active-Filter Rectifier: Starting from Fig. 12(a) and following a circuit concept known from passive injection networks [14], [52], the two inductors L_+ and L_- could be lumped together into a single inductor L_{Y} lying in the injection path. The resulting circuit structure is shown in Fig. 14, [16], [17], [53]. The output diodes D_+ and D_- can now be omitted, since a simultaneous switching on of the transistors S_+ or S_- would lead to a short-circuiting of the mains, in contrast to Fig. 12, and is thus not allowed.

Accordingly, the systems show a relatively low implementation effort, however, at the expense of a missing output voltage control. As can be immediately seen from the absence of diodes D_+ and D_-, the output voltage is now determined directly by the diode bridge and, hence, exhibits a six-pulse shape. However, as will be shown below, assuming a constant power load, the possibility of impressing sinusoidal mains phase currents remains. Thus, the system does not provide the full functionality of an output voltage-regulated PFC rectifier, but the function of a passive rectifier with an integrated active filter and hence should be called a *hybrid third harmonic current injection active-filter rectifier*.

If a load with constant power consumption is supplied, there results a load current varying in antiphase to the six-pulse rectifier output voltage. As shown below, this leads to a sinusoidal shape of all mains phase currents after overlaying with the injection current.

Consider a 60° interval of the mains period with $u_{\mathrm{aN}} > u_{\mathrm{bN}} > u_{\mathrm{cN}}$ as in Section IV-A1. For the current to be injected into phase b

$$\bar{i}_{\mathrm{Y}} = -\bar{i}_{\mathrm{b}} = -G^* u_{\mathrm{bN}} \tag{16}$$

applies. The mains frequency voltage drop across the inductor L_{Y} can in a first approximation be neglected for the formation of $\bar{i}_{\mathrm{Y}}$

$$\bar{u}_{\mathrm{L_Y}} = 0\,. \tag{17}$$

Accordingly, we have for the voltage to be formed at the output of the bridge-leg

$$\bar{u}_{\mathrm{YN}} = \bar{u}_{\mathrm{bN}}\,. \tag{18}$$

If in any case one of the transistors S_+ or S_- is switched ON, $\alpha_+ + \alpha_- = 1$ applies for the relative switch-on times or $\alpha_- = 1 - \alpha_+$ and hence, for the voltage formation of the bridge-leg

$$\bar{u}_{\mathrm{L_Y}} = \alpha_+ u_{\mathrm{aN}} + (1-\alpha_+)\, u_{\mathrm{cN}} = \alpha_+ u_{\mathrm{ac}} + u_{\mathrm{cN}}\,. \tag{19}$$

Correspondingly, there follows the duty cycle α_+ with (19) as

$$\alpha_+ = \frac{u_{\mathrm{bc}}}{u_{\mathrm{ac}}} \tag{20}$$

and thus for the current in S_+

$$\bar{i}_{\mathrm{S+}} = \alpha_+ i_{\mathrm{Y}} = -\alpha_+ i_{\mathrm{b}} = -\alpha_+ G^* u_{\mathrm{bN}} = -G^* u_{\mathrm{bN}} \frac{u_{\mathrm{bc}}}{u_{\mathrm{ac}}}\,. \tag{21}$$

Considering the fundamental input currents that have to be generated at the input

$$\begin{aligned} \bar{i}_{\mathrm{a}} &= G^* u_{\mathrm{aN}} \\ \bar{i}_{\mathrm{b}} &= G^* u_{\mathrm{bN}} \\ \bar{i}_{\mathrm{c}} &= G^* u_{\mathrm{cN}} \end{aligned} \tag{22}$$

the low-frequency component of the current consumption of the constant power load can be expressed via

$$i = \frac{P_{\mathrm{o}}}{u_{\mathrm{ac}}} = \frac{\bar{i}_{\mathrm{a}} u_{\mathrm{ac}} + \bar{i}_{\mathrm{b}} u_{\mathrm{bc}}}{u_{\mathrm{ac}}} = G^* \frac{u_{\mathrm{aN}} u_{\mathrm{ac}} + u_{\mathrm{bN}} u_{\mathrm{bc}}}{u_{\mathrm{ac}}} \tag{23}$$

$$= G^* \left(u_{\mathrm{aN}} + u_{\mathrm{bN}} \frac{u_{\mathrm{bc}}}{u_{\mathrm{ac}}} \right)\,. \tag{24}$$

For the resultant low-frequency current component drawn from phase a, there, then, follows with (21)

$$\bar{i}_{\mathrm{a}} = i - \bar{i}_{\mathrm{S+}} = G^* u_{\mathrm{aN}} \tag{25}$$

directly the desired (sinusoidal) waveform proportional to the mains voltage. Furthermore, there applies with (16), (25)

$$i_{\mathrm{a}} + i_{\mathrm{b}} + i_{\mathrm{c}} = 0 \tag{26}$$

and $u_{\mathrm{aN}} + u_{\mathrm{bN}} + u_{\mathrm{cN}} = 0$ for phase c

$$\bar{i}_{\mathrm{c}} = G^{*} u_{\mathrm{cN}} \tag{27}$$

so that the sinusoidal shape of all phase currents has been proved.

It must be emphasized that the circuit in Fig. 14(a) allows a sinusoidal regulation of the mains currents only in case a converter output stage, e.g., in the form of a dc–dc converter or a PWM inverter stage, is present that assures constant power consumption. The implementation effort of this concept should, therefore, be evaluated only with regard to the overall system.

Furthermore, it should be noted that the waveform of i required for the formation of a sinusoidal mains current only results if no smoothing capacitor (of higher capacitance) is connected between constant power load and rectifier stage. Load variations are, thus, passed on directly to the mains.

3) Δ-Switch Rectifier: If the circuit in Fig. 10(c) is extended with a third bridge-leg and a delta-connection of four-quadrant switches is added with respect to the operating principle and the three-phase symmetry, there follows the topology in Fig. 15(a) of the Δ-switch rectifier [54]–[56]. The four-quadrant switches enable to influence the conduction state of the diode rectifier and, thus, to control the ac-side voltage formation via PWM. The Δ-switch rectifier is an active PFC rectifier circuit since the commutation of the diode bridge occurs, in contrast to the circuit in Fig. 12, at switching frequency.

Similar to single-phase PFC rectifier circuits, the voltage formed at the input of a rectifier bridge-leg, e.g., $\bar{u}_{\bar{\mathrm{a}}M'}$ (M' designates a virtual midpoint of the output voltage), depends on the switching state of the (entire) converter and on the direction of the phase current i_{a}. This does not represent a limitation since a current i_{a} in phase with the mains voltage u_{aN} has to be impressed. Neglecting the voltage drop across the input inductor $u_{\mathrm{aN}} \approx \bar{u}_{\bar{\mathrm{a}}\mathrm{N}}$ has to be ensured. Therewith, $i_{\bar{\mathrm{a}}} = G^{*} u_{\mathrm{aN}}$ and $\bar{u}_{\bar{\mathrm{a}}\mathrm{N}}$ always have the same polarity.

Except for a simultaneous switch on of all four-quadrant switches ($s_{\bar{\mathrm{a}}\bar{\mathrm{b}}} = s_{\bar{\mathrm{b}}\bar{\mathrm{c}}} = s_{\bar{\mathrm{c}}\bar{\mathrm{a}}} = 1$), one phase terminal, e.g., $\bar{a}$, is always connected with the positive or negative output voltage bus p or n. Accordingly, the circuit shows a two-level characteristic with regard to the voltage formation. As is immediately clear considering the diode rectification on the input side, the output voltage has to be selected according to

$$U_{\mathrm{pn}} > \sqrt{2}\, U_{\mathrm{N,ll,rms}} \ . \tag{28}$$

In the case of a failure of a mains phase, the two four-quadrant switches associated with the phase that failed have to be permanently disabled. Then, again a single-phase PFC rectifier circuit with an ac-side switch is present, which operates, however, from a line-to-line voltage, but still allows a regulation of the output voltage and a sinusoidal impression of the mains currents.

It is interesting to understand that the operating range of the Δ-switch rectifier is not restricted to ohmic fundamental mains behavior (as could be expected due to the diode rectifier) but allows the formation of current phase displacements in the

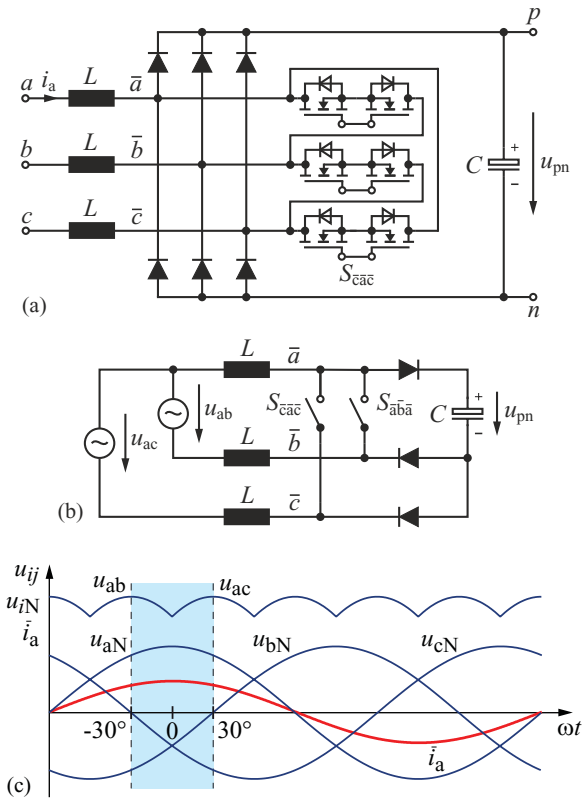

Fig. 15. (a) Circuit topology of the Δ-switch rectifier [54]. Also, a bridge configuration of six transistors with antiparallel diodes and short-circuited output terminals could be used instead of a delta-connection of four-quadrant switches. (b) Equivalent circuit of the system for $i_{\mathrm{a}} > 0$, $i_{\mathrm{b}} < 0$, $i_{\mathrm{c}} < 0$, i.e., for $\varphi_{\mathrm{N}} = (-30°, +30°)$. (c) Waveforms of the mains phase voltages, local average phase current $\bar{i}_{\mathrm{a}}$, and sections of the line-to-line voltages.

angular interval

$$\Phi = (-30°, +30°). \tag{29}$$

This can be clarified by a more detailed analysis of the conduction states of the system, which may be restricted to a 60° interval due to the symmetry of the three-phase mains system. The equivalent circuit of the active part of the Δ-switch rectifier is shown in Fig. 15(b) for $i_{\mathrm{a}} > 0, i_{\mathrm{b}} < 0, i_{\mathrm{c}} < 0$. It is assumed that only the four-quadrant switches connected to the phase with the largest absolute voltage value is switched [55].

For the impression of i_{b} and i_{c}, $S_{\bar{\mathrm{a}}\bar{\mathrm{b}}}$ and $S_{\bar{\mathrm{a}}\bar{\mathrm{c}}}$ are switched such that $\bar{u}_{\bar{\mathrm{a}}\bar{\mathrm{c}}}$ and $u_{\bar{\mathrm{a}}\bar{\mathrm{b}}}$ compensate the line-to-line voltages $u_{\mathrm{ac}} > 0$ and $u_{\mathrm{ab}} > 0$. The voltages $\bar{u}_{\bar{\mathrm{a}}\bar{\mathrm{c}}}$ and $\bar{u}_{\bar{\mathrm{a}}\bar{\mathrm{b}}}$ can be formed for the given polarities of the currents. However, as a result of the phase displacement between the phase quantities and the line-to-line quantities of ±30° (compare, e.g., u_{aN} and u_{ab} or u_{aN} and u_{ac}) $u_{\mathrm{ac}} > 0$ and $u_{\mathrm{ab}} > 0$ applies, not only for $\varphi_{\mathrm{N}} = (-30°, 30°)$ but also for $\varphi_{\mathrm{N}} = (-60°, 60°)$. Therewith, the balance of the voltages $u_{\mathrm{ac}} \approx \bar{u}_{\bar{\mathrm{a}}\bar{\mathrm{c}}} > 0$ and $u_{\mathrm{ab}} \approx \bar{u}_{\bar{\mathrm{a}}\bar{\mathrm{b}}} > 0$ can be also achieved for phase voltages with a displacement of ±30° against the phase current system.

The voltage reference values formed at the output of the phase current controllers are converted with a Y-Δ transformation into

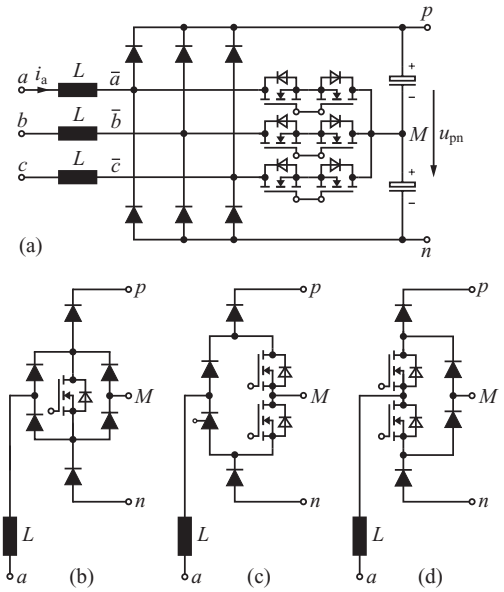

Fig. 16. (a) Circuit topology of the original VIENNA rectifier [44]. (b)–(d) Alternative bridge-leg structures, whereas the bridge-leg variant (b) requires only three transistors but shows higher conduction losses due to the series-connected diodes [57]; (c) [58] is advantageous concerning precharging the output capacitor at start-up [57] (after the precharge interval the thyristor is gated, thus, a parallel path with precharging resistor and series diode is bypassed); (d) [59] allows a further reduction of the conduction losses compared to the topology in (c).

the effectively adjustable line-to-line voltage reference values

$$\begin{aligned} u^*_{\bar{a}\bar{b}} &= u^*_{\bar{a}N} - u^*_{\bar{b}N} \\ u^*_{\bar{b}\bar{c}} &= u^*_{\bar{b}N} - u^*_{\bar{c}N} \\ u^*_{\bar{c}\bar{a}} &= u^*_{\bar{c}N} - u^*_{\bar{a}N}. \end{aligned} \tag{30}$$

The polarity of the phase currents or phase voltages, i.e., the information of the actual 60° sector of the mains period has, then, to be considered for the control of the individual power transistors, however, no sector dependent switch over of the entire control structure is required. This results in a higher input current quality as a switch over of the control, potentially causes current distortions at the switching instants.

4) VIENNA *Rectifier:* If the delta(Δ)-connection of the four-quadrant control switches of the Δ-switch rectifier is replaced by a star-connection, and the star-point of the switch arrangement is connected to a capacitively formed midpoint M of the output voltage in terms of highest possible symmetry, an active three-level PWM rectifier system (cf., Fig. 16(a), [44], [57]), known as VIENNA rectifier, results. Functionally equivalent alternative implementations of the bridge-leg structure with a lower blocking voltage stress of the power diodes are depicted in Fig. 16(b)–(d) [57]–[59].

As for the Δ-switch rectifier, the ac-side voltage formation of the system is again dependent on the sign of the phase currents. However, the rectifier phase input, e.g., $\bar{a}$, now can be also connected to the midpoint M of the output voltage besides the positive and the negative output voltage bus. Thus, three voltage levels are available for the formation of $\bar{u}_{\bar{a}M}$, which justifies the designation of the system as a three-level converter.

A major advantage of the three-level characteristic is that for the selection of the blocking voltage capability of the power transistor only half of the peak value of the line-to-line voltage and not the total value is relevant. Furthermore, as a result of the higher number of levels of $\bar{u}_{\bar{a}M}$, the difference $u_{aN} - u_{\bar{a}N}$ remains limited to small values. Thus, a smaller mains current fundamental ripple results [cf., (2)], and/or the value of the input (boost) inductances can be reduced. In addition, as a result of the lower switched voltage, a lower conducted EMI noise level is also generated.

In analogy to the Δ-switch rectifier

$$U_{pn} > \sqrt{2}\, U_{N,ll,rms} \tag{31}$$

applies for the output voltage range of the system and

$$\Phi = (-30^\circ, +30^\circ) \tag{32}$$

for the phase displacement range of the mains voltage and the mains current fundamental in case a high-output voltage $U_{pn} > 2\sqrt{2}\, U_{N,ll,rms}$ and a small boost inductance are assumed. The phase displacement range is increasingly reduced to pure ohmic mains behavior ($\Phi = 0$) [56], [57] for lower output voltage values, i.e., for $\sqrt{2}\, U_{N,ll,rms} < U_{pn} < 2\sqrt{2}\, U_{N,ll,rms}$. Similar to the Δ-switch rectifier in the case of a phase loss, the VIENNA rectifier also can still be operated at a reduced output power and at the same output voltage and with sinusoidal input currents in the remaining phases [60]–[62].

The output voltages of the system can be loaded asymmetrically, as was shown in the analysis in [63]. However, the admissible degree of asymmetry depends on the mains voltage level. High degrees of asymmetry are only possible for high-output voltages.

A state-of-the-art hardware demonstrator of the VIENNA rectifier is shown in Fig. 17. The switching frequency of the system is $f_P = 250$ kHz. Such a high-switching frequency, however, is only useful if an extremely low THD_i of the input currents has to be achieved at high mains frequencies (e.g., for More Electric Aircraft [56], $f_N = 360\,\text{Hz} \ldots 800\,\text{Hz}$).

5) Hybrid Half-Controlled/Active Full-Controlled Six-Switch PFC AC/DC Bridge Circuit: If instead of the conventional single-phase PFC rectifier structure bridgeless (or dual-boost) converter topology in Fig. 10(b) is extended to three-phases, a half-controlled hybrid phase-symmetrical rectifier circuit shown in Fig. 18(a) results.

This circuit topology does not allow to impress a sinusoidal input current within the entire mains period because of the lack of bridge-symmetry. If, e.g., a 60° interval with $u_{aN} > 0$ and $u_{bN}, u_{cN} < 0$, i.e., an angular interval $\varphi_N = (-30^\circ, 30^\circ)$ of the mains period is considered [cf., Fig. 19(a)] and phase currents with identical signs as the corresponding mains phase voltage are assumed, only the switching-off of $S_{\bar{a}n}$ would cause a commutation of i_a to $D_{\bar{a}p}$. In the phases b and c, the antiparallel diodes $D_{n\bar{b}}$ and $D_{n\bar{c}}$ would remain conductive, independent of the switching state of the transistors $S_{\bar{b}n}$ and $S_{\bar{c}n}$.

Therefore, a sinusoidal current impression is possible only for those 60° intervals in which two mains phase voltages have a

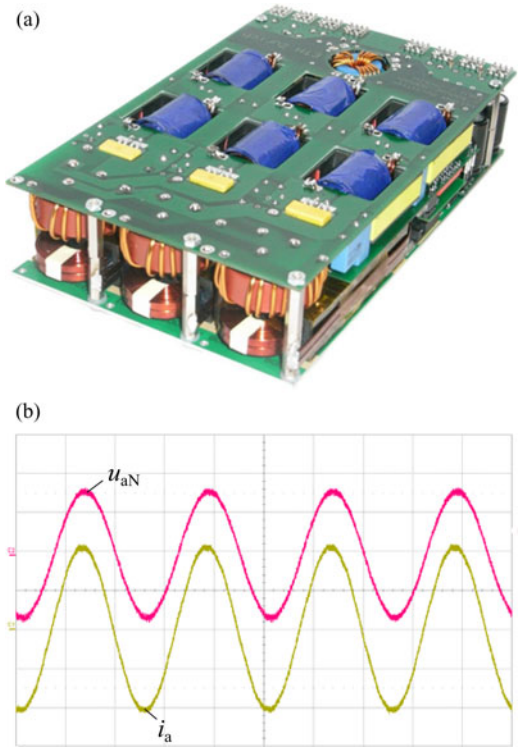

Fig. 17. (a) Hardware demonstrator of a 10-kW VIENNA rectifier (dimensions: 195 mm × 120 mm × 43 mm; power density: $\rho = 10\,\mathrm{kW/dm^3} = 164\,\mathrm{W/in^3}$). (b) Measured phase current i_a ($\mathrm{THD_i} = 1.6\%$) and corresponding mains phase voltage u_{aN}. Operating parameters: mains rms line-to-line voltage $U_{N,ll,rms} = 400\,\mathrm{V}$, mains frequency $f_N = 800\,\mathrm{Hz}$, output voltage $U_{pn} = 800\,\mathrm{V}$, and switching frequency $f_P = 250\,\mathrm{kHz}$. Scales: 200 V/div, 10 A/div, and 0.5 ms/div.

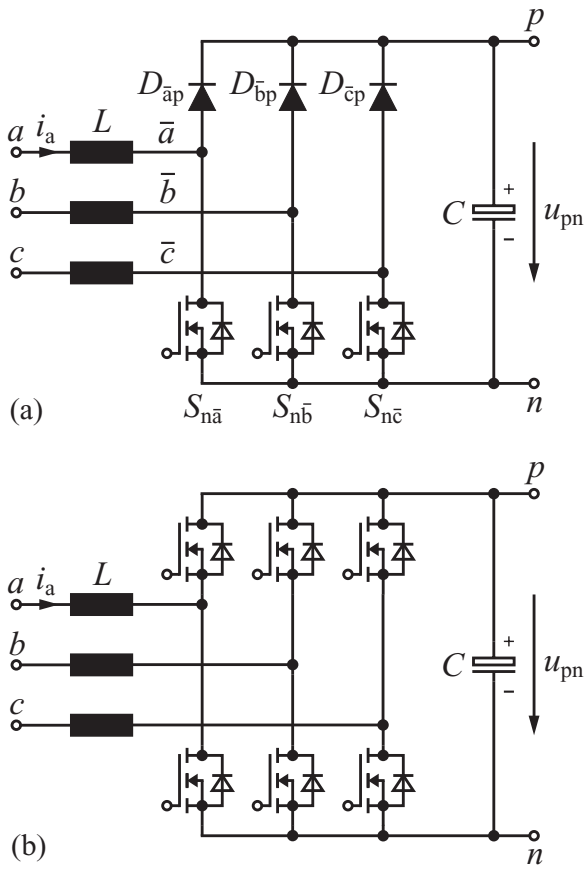

Fig. 18. (a) Half-controlled (hybrid) boost-type three-phase ac–dc bridge circuit. (b) Full-controlled active three-phase ac–dc bridge circuit (bidirectional six-switch active PFC rectifier).

positive sign, thus when, e.g., $u_a, u_b > 0$, $u_c < 0$, or $i_{\bar{a}}, i_{\bar{b}} > 0$, $i_{\bar{c}} < 0$ applies [cf., $\varphi_N = (30°, 90°)$, Fig. 19(c)]. By switching ON $S_{n\bar{a}}$ or $S_{n\bar{b}}$, $\bar{a}$ or $\bar{b}$ can then be connected to the negative output voltage bus n and i_a or i_b increased. At the switch-off of $S_{N\bar{a}}$ or $S_{N\bar{b}}$, the corresponding freewheeling diode $D_{\bar{a}p}$ or $D_{\bar{b}p}$ becomes conducting. Thus, a positive potential is applied to $\bar{a}$ or $\bar{b}$, and the corresponding phase currents are reduced. Therewith, either an increase or decrease of two phase currents and consequently a sinusoidal current waveform is achievable. The third phase current then also shows a sinusoidal shape as a result of $i_a + i_b + i_c = 0$.

In summary, a sinusoidal current shape can be achieved only in sections of the mains period. The function of the circuit is, hence, essentially limited to output voltage regulation, whereby by using the simple control procedure described in [64], at least a block-shaped current waveform, comparable to passive rectifiers, may be realized.

It should be noted that to simplify matters, all transistors could also be switched synchronously with a duty cycle constant over the mains period and the system operated in DCM. The input current shape would then be identical to that in Fig. 11(d). As an advantage, lower conduction losses would occur but at the cost of a higher implementation effort.

Voltage regulation and sinusoidal current impression requires an extension of the circuit in Fig. 18(a) to bridge symmetry, i.e., the addition of three further transistors antiparallel to the freewheeling diodes of the positive bridge half. There then results the six-switch converter structure shown in Fig. 18(b), which is employed, e.g., for supplying of the voltage dc-link of variable speed drives.

Since for a switched-on transistor the current in any case flows over this transistor or its antiparallel diode, the system allows, in each phase, a voltage formation independent of the current. At the input of each rectifier bridge-leg, a positive or a negative voltage may be generated referred to the virtual output voltage midpoint. Thus, the bridge-legs exhibit a two-level characteristic and, hence, allow the impression of sinusoidal phase currents of any phase displacement relative to the mains voltage. In particular, the current may also be led in antiphase to the mains voltage, i.e., power may be fed back into the mains. This inverter operating mode is, e.g., employed in variable speed ac machine drives to feed braking energy back into the mains, and represents the main energy flow direction for supplying an ac machine from a voltage dc-link.

With regard to the level of the output voltage

$$U_{pn} > \sqrt{2} U_{N,ll,rms} \tag{33}$$

is required, the same as for the systems in Figs. 15(a) and 16. Furthermore, the system can deal with a mains phase failure,

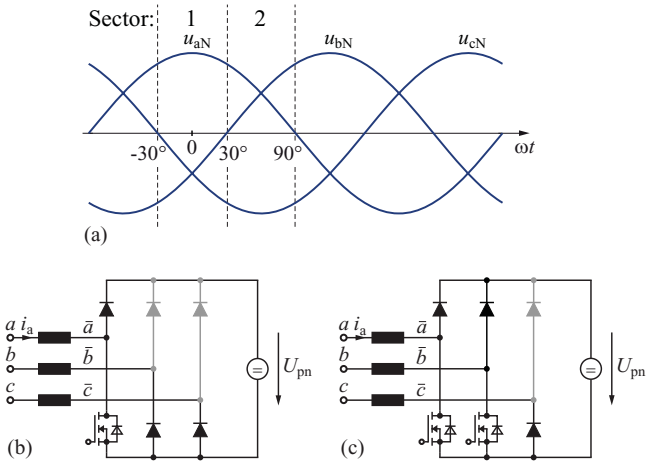

Fig. 19. (a) Time behavior of the phase voltages within a mains period. (b) Active part of the system for sector 1 ($u_{aN} > 0$, $u_{bN}, u_{cN} < 0$) with the possibility of controlling only one phase current. (c) Active part of the system for sector 2 ($u_{aN}, u_{bN} > 0$, $u_{cN} < 0$) with the possibility of controlling two-phase currents, i.e., all phase currents.

thus representing a mains interface that can be used in an extremely flexible manner. Hence, the entire circuit structure is also commercially available as a power module (generally denominated as "sixpack" power module) and is widely used in industry.

It should be emphasized that the circuit has a relatively simple structure, despite the high functionality, i.e., in particular, the bidirectionality does not result in an increase in the number of switches compared with the unidirectional structures derived previously. This becomes especially clear on using reverse conducting (RC)-IGBTs, which apart from the power transistor, also include the antiparallel freewheeling diode in one chip. The same applies (in future), e.g., for SiC JFETs (in cascode connection). The circuit is, thus, of particular interest, despite the limitation made here to unidirectional systems as the wide phase angle range may also be exploited in the purely rectifier mode, e.g., for reactive power compensation.

6) Discussion: According to Section IV-A1, the implementation of a three-phase boost-type PFC rectifier is possible with a current injection concept based on passive-diode rectification or, according to Sections IV-A2– IV-A4, by control of the conduction state of a diode bridge with turn-off power semiconductors, which allows a direct impression of sinusoidal ac currents.

The direct ac current impression is preferable compared with the impression of two dc currents (in combination with a current injection into the third phase) for an industrial system since a switching at the sector borders, potentially causing distortions, is not required. In addition, active rectifier systems are not limited to a purely ohmic fundamental mains behavior, therewith, e.g., the capacitive reactive power of the EMI input filter can be (partly) compensated, or in general a higher flexibility for the current control is given.

Thus, for the comparative evaluation in [65], only the Δ-switch rectifier, the VIENNA rectifier and the (bidirectional) six-switch boost-type PFC rectifier are considered. The Δ-switch rectifier could here be also omitted with regard to the system complexity. Given by its structure, however, the system cannot generate a short-circuit of the output voltage in the case of a faulty control of the power transistors. Therewith, an advantage is given regarding the operational safety compared with the six-switch converter. The evaluation of the system, furthermore, is reasonable in terms of completeness of the analysis.

B. Systems With Buck-Type Characteristic

As single-phase buck-type ac–dc converters do not enable to provide sinusoidal currents over the entire mains period [24], the derivation of buck-type PFC rectifier structures has to refer directly to three-phase diode rectifier circuits with dc-side inductor [cf., Fig. 2(b)]. The diode bridge has to be extended with turn-off elements by considering phase- and bridge-symmetry requirements, such that the mains phases to be connected with the dc side can be arbitrarily selected. Alternatively, also a system based on the injection principle could be conceptualized with reference to Section IV-A1.

1) Active Six-Switch Buck-Type PFC Rectifier: A power transistor has to be added in series to each diode in the circuit shown in Fig. 2(b) to enable a full, i.e., a voltage-independent controllability of the power transfer. The resultant converter structure is shown in Fig. 20(a), which is known from current dc-link converters used for drive systems [66]. The diode–transistor series combinations represent, here, unidirectional, bipolar blocking switches, which can also be replaced by RB-IGBTs in terms of a reduction of the conduction losses. However, a limitation of the switching frequencies to relatively low values (in the range of 10 kHz) would then be required due to the relatively high switching losses [67].

If a transistor of the positive bridge half, e.g., transistor $S_{\bar{a}p}$, and a transistor of the negative bridge half, e.g., $S_{n\bar{c}}$, are switched ON, the output inductor current I is drawn from phase a and fed back into phase c

$$\begin{aligned} i_a &= +I \\ i_b &= 0 \\ i_c &= -I \end{aligned} \tag{34}$$

[cf., Fig. 20(b)]. In addition, the line-to-line voltage u_{ac} is switched to the output, i.e., is used for the formation of the output voltage

$$u_{pn} = u_{\bar{a}N} - u_{\bar{c}N} = u_{\bar{a}\bar{c}} = u_{ac}. \tag{35}$$

If solely both transistors of a bridge-leg are switched ON, $i_a = i_b = i_c = 0$ applies and $u = 0$, i.e., the system is in a freewheeling state. The conduction losses in the freewheeling state could be reduced by implementation of an explicit freewheeling diode.

By proper modulation, the output current i can, thus, be distributed to the three phases in such a manner that after low-pass filtering of the pulsewidth modulated discontinuous input currents $i_{\bar{a}}$, $i_{\bar{b}}$, $i_{\bar{c}}$ sinusoidal mains currents result (in Fig. 20(a), only the filter capacitors C_F of the EMI filter on the mains side are shown). Furthermore, the output voltage, which is formed by low-pass filtering of u with the output inductor L and the

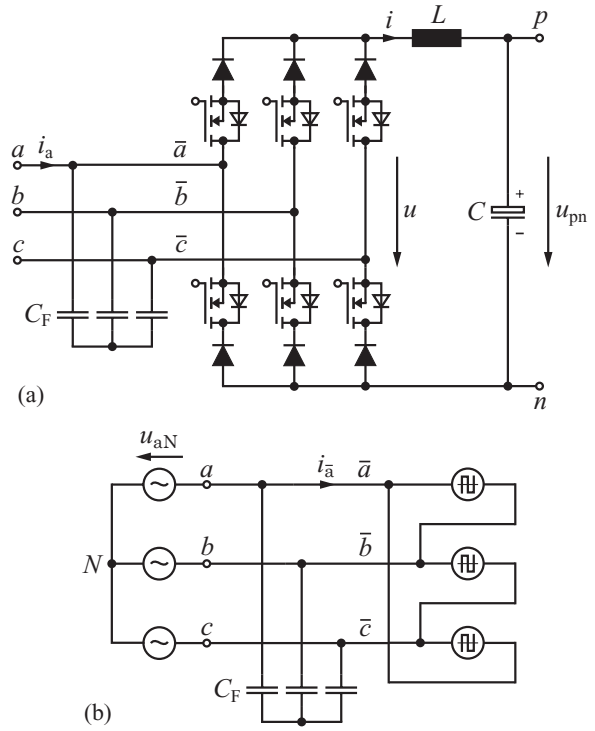

Fig. 20. (a) Circuit topology of the active six-switch buck-type PFC rectifier. (b) Equivalent circuit of ac part of the system. Note that if power transistors were only implemented in the positive or negative bridge half, a circuit analogous to Fig. 18(a) would result, which also would not allow for a sinusoidal current impression due to the limited controllability.

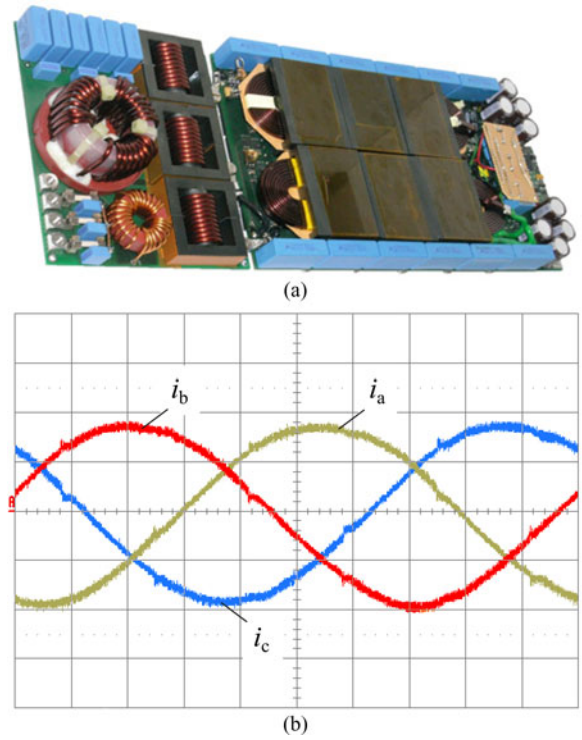

Fig. 21. (a) Hardware demonstrator of a 6-kW active six-switch buck-type PFC rectifier (dimensions: 418 mm × 155 mm × 31 mm; power density: $\rho = 2.2\,\mathrm{kW/dm^3} = 36\,\mathrm{W/in^3}$). (b) Time behavior of the phase currents within a mains period. Operating parameters: rms line-to-line voltage $U_{\mathrm{N,ll,rms}} = 400\,\mathrm{V}$, mains frequency $f_{\mathrm{N}} = 50\,\mathrm{Hz}$, dc output voltage $U_{\mathrm{pn}} = 400\,\mathrm{V}$, and switching frequency $f_{\mathrm{P}} = 18\,\mathrm{kHz}$. The rectifier enables an extremely high nominal efficiency of $\eta_{\mathrm{nom}} = 98.9\%$ [70] although there are always four power semiconductor in the current path (two diode–MOSFET series connections). Scales: 5 A/div, 2 ms/div.

output capacitor C, can be adjusted with the relative duration of the freewheeling state starting from zero to values

$$U_{\mathrm{pn}} < \sqrt{\frac{3}{2}}\, U_{\mathrm{N,ll,rms}}. \tag{36}$$

The limited output voltage range is explained by the fact that two line-to-line voltages have to be used in each pulse period for the formation of the output voltage in order to supply each mains phase with current. In order to maximize the achievable output voltage, here, always the two largest voltages, e.g., $u_{\bar{a}\bar{c}}$ and $u_{\bar{a}\bar{b}}$ are selected [valid within a 60° interval of the mains period $\varphi_{\mathrm{N}} = (-30°, +30°)$, cf., Fig. 15(c)]. Both voltages have a phase displacement of 60°. Therefore, only voltage values $u_{\bar{a}\bar{c}} = u_{\bar{a}\bar{b}} = \sqrt{3/2}\, U_{\mathrm{N,ll,rms}}$ are available for the pulse period at the intersection of both voltages. Correspondingly, the output voltage range is defined by (36). The full controllability of the system generally allows an arbitrary phase displacement between the mains current and the mains voltage of

$$\Phi = (-180°, +180°). \tag{37}$$

However, with an increasing phase displacement Φ, the line-to-line voltages switched to the output have lower instantaneous values, and/or

$$U_{\mathrm{pn}} < \sqrt{\frac{3}{2}}\, U_{\mathrm{N,ll,rms}} \cos(\Phi) \tag{38}$$

applies. Correspondingly, e.g., for $\Phi = 90°$ follows $U_{\mathrm{pn}} = 0$, as is immediately clear considering the power balance between the ac and the dc side. The output voltage range (36) is, thus, only valid for $\Phi = 0°$ and/or in order to ensure a wide output voltage range, the phase displacement Φ has to be limited to small values [68].

Note that according to (37), for the circuit in Fig. 20(a), the reversal of the power flow direction demands a change of the output voltage. A reversal of the power flow direction at the same polarity of the output is only possible by extension of the circuit structure with antiparallel transistors to the diodes [69].

A hardware demonstrator of the rectifier system is presented in Fig. 21 [70]. The efficiency of the system, implemented with 900-V superjunction MOSFETs and SiC Schottky diodes ($f_{\mathrm{P}} = 18\,\mathrm{kHz}$) equals 98.9% at the nominal operating point. This clearly shows, that with an appropriate semiconductor effort, despite the implementation of the switches as diode–transistor series connection, very high efficiencies are achievable.

2) Active Three-Switch Buck-Type PFC Rectifier: As an alternative to Fig. 20, the selection of the conducting phases is also possible with four-quadrant switches arranged on the ac side of the bridge rectifier. The four-quadrant switches can then be integrated into the bridge-leg structure as shown in Fig. 22(a)–(c). The resulting three-switch buck-type PFC rectifier system is depicted in Fig. 22(d).

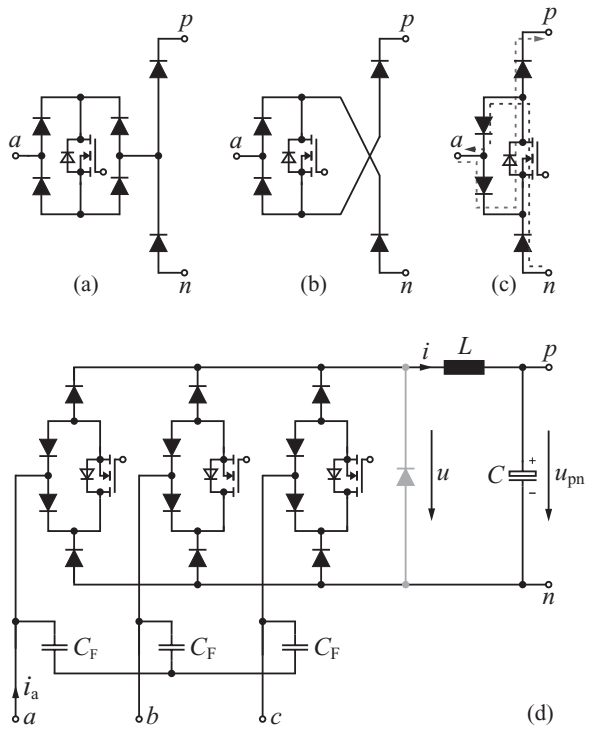

Fig. 22. Derivation of the circuit topology of the active three-switch buck-type PFC rectifier. A four-quadrant switch is formed by a diode bridge and a dc-side power transistor is inserted on the ac side in (a). After merging series connected diodes and redrawing, the bridge-leg structure in (c) results, and/or the three-phase circuit topology in (d).

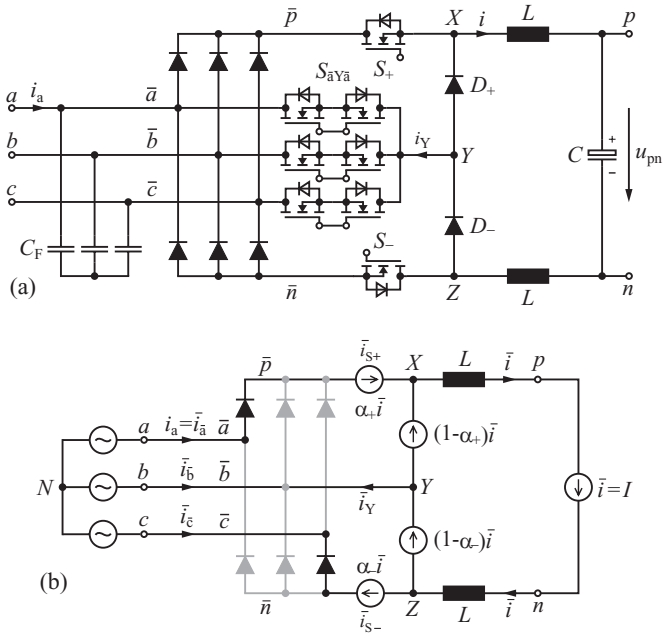

Fig. 23. a) Basic structure of the SWISS Rectifier. b) Local average equivalent circuit of the active part of the system for $u_{aN} > u_{bN} > u_{cN}$.

Due to the reduction of the number of switches and/or higher number of diodes, higher conduction losses result. On the other hand, the installed chip area of the power transistors is better utilized. However, as a result of the lower number of switches, the controllability is limited compared with Fig. 20. There is no other possibility given for a reversal of the power flow direction, as can be immediately verified with Fig. 22(a). Furthermore, only the current conducting bridge-legs but not directly the current conducting diodes are definable. The conduction state, thus, adjusts depending on the polarity of the voltages at the activated bridge-legs.

A restriction of the operating range to

$$\Phi = (-30^\circ, +30^\circ) \tag{39}$$

results, as is shown by a more detailed analysis, which, however, is of minor importance in view of the preferred ohmic operation as a consequence of (38). A figurative explanation of (39) is possible in a similar manner as for the boost-type Δ-switch rectifier [cf., Fig. 15(c)] with the $\pm 30^\circ$ phase displacement between the phase quantities and the line-to-line quantities, however, is not shown here for the sake of brevity. The output voltage range for $\Phi = 0^\circ$ is still given by

$$U_{\rm pn} < \sqrt{\frac{3}{2}} U_{\rm N,ll,rms}. \tag{40}$$

The control scheme of the six-switch buck-type PFC rectifier can be also applied to the three-switch system. The switching signals of the transistors then have to be generated by OR-connection of the switching signals of the power transistors of the respective bridge-legs of the six-switch buck-type PFC topology.

*3) Hybrid Current Injection Buck-Type (*SWISS*) PFC Rectifier:* As an alternative to the direct control of the current formation of a three-phase diode bridge, a three-phase PFC rectifier can also be implemented, according to the concept of third harmonic current injection described in Section IV-A1 for boost-type systems. Then, only the dc–dc boost converters of the circuit in Fig. 11 have to be replaced by buck converters. The resultant circuit is shown in Fig. 23(a). To the knowledge of the authors, this system has not yet been described in the literature, presumably due to the general focus in research on systems with boost-type characteristic. In the following, the circuit topology is, thus, designated as SWISS rectifier [4], [71].

Contrary to the circuits according to Sections IV-B1–IV-B2, the rectifier diodes of the system are not commutated with switching frequency. Correspondingly, the conduction losses can be reduced by employing devices with a low forward voltage drop (and a higher reverse recovery time). As for the boost-type system, the current injection is performed again with four-quadrant switches into the phase with the currently smallest absolute voltage value. In this context, it should be mentioned that with a passive injection network, a current injection into all three phases is possible. Such a system was proposed in [15] and is, as described in Section IV-A1, also known for boost-type systems. However, in consideration of the large volume of the passive injection network and the higher injection current, this approach is not discussed further in this paper.

For the proof of the sinusoidal controllability of the mains currents, again a 60° interval of the mains period with $u_{\rm aN} >$

$u_{\mathrm{bN}} > u_{\mathrm{cN}}$ or $\varphi_{\mathrm{N}} = (0°, 60°)$ is considered. The active part of the circuit in this mains sector is depicted in Fig. 23(b).

The rectifier system should represent a symmetric three-phase load of (fundamental) phase conductance G^* to the mains. Accordingly, the local average values of the (discontinuous) input currents may be written as

$$\begin{aligned} \overline{i}_{\bar{\mathrm{a}}} &= G^* u_{\mathrm{aN}} \\ \overline{i}_{\bar{\mathrm{b}}} &= G^* u_{\mathrm{bN}} \\ \overline{i}_{\bar{\mathrm{c}}} &= G^* u_{\mathrm{cN}} \end{aligned} \tag{41}$$

($u_{\mathrm{iN}} = u_{\bar{\mathrm{i}}\mathrm{N}}$). The reference output current I^*, to be impressed by the buck converter, is then given under the assumption of a symmetrical three-phase mains system by

$$I^* = \frac{3}{2} G^* \frac{\hat{U}_{\mathrm{N}}^2}{U_{\mathrm{pn}}} \tag{42}$$

($\hat{U}_{\mathrm{N}}$ designates the amplitude of the phase voltages, U_{pn} is the output voltage). An ideal output current controller and/or $\overline{i} = I = I^*$ is assumed for further considerations. The currents in the phases a and c are impressed by a respective switching (PWM) of S_+ and S_-

$$\alpha_+ I = \overline{i}_{\bar{\mathrm{a}}} \qquad \alpha_- I = -\overline{i}_{\bar{\mathrm{c}}} \tag{43}$$

whereby the duty cycles result with (41), (42), and (43) as

$$\alpha_+ I = \frac{2}{3} \frac{U_{\mathrm{pn}}}{\hat{U}_{\mathrm{N}}^2} u_{\mathrm{aN}} \qquad \alpha_+ I = -\frac{2}{3} \frac{U_{\mathrm{pn}}}{\hat{U}_{\mathrm{N}}^2} u_{\mathrm{cN}}. \tag{44}$$

Considering the partitioning of the current in the node Y and $i_{\mathrm{a}} + i_{\mathrm{b}} + i_{\mathrm{c}} = 0$ or $\overline{i}_{\bar{\mathrm{a}}} + \overline{i}_{\bar{\mathrm{b}}} + \overline{i}_{\bar{\mathrm{c}}} = 0$, the injection current

$$\overline{i}_{\mathrm{Y}} = (1 - \alpha_-)\, I - (1 - \alpha_+)\, I = \overline{i}_{\bar{\mathrm{a}}} + \overline{i}_{\bar{\mathrm{c}}} = -\overline{i}_{\bar{\mathrm{b}}} \tag{45}$$

results. Thus, the correct current is injected into the third phase (here phase b). For the formation of the output voltage,

$$\bar{u}_{\mathrm{XZ}} = \alpha_+ u_{\mathrm{aN}} + (1 - \alpha_+)\, u_{\mathrm{bN}} - \left(\alpha_- u_{\mathrm{cN}} + (1 - \alpha_-)\, u_{\mathrm{bN}}\right) \tag{46}$$

is relevant. After simplification, the output voltage may be written as

$$\bar{u}_{\mathrm{XZ}} = \alpha_+ u_{\mathrm{ab}} - \alpha_- u_{\mathrm{cb}}. \tag{47}$$

A multiplication of (47) with I results in

$$\bar{u}_{\mathrm{XZ}} I = \overline{i}_{\mathrm{a}} u_{\mathrm{ab}} + \overline{i}_{\mathrm{c}} u_{\mathrm{cb}} = \bar{p} = P \tag{48}$$

the instantaneous power $\bar{p}$, which under the assumption of symmetrically loaded mains shows a constant value $\bar{p} = P$. Accordingly, at a constant current I, also a constant voltage $\bar{u}_{\mathrm{xz}}$ and thus due to $\bar{u}_{\mathrm{L}} = 0$ a constant output voltage $\bar{u}_{\mathrm{pn}} = U_{\mathrm{pn}}$ is generated.

As the previous derivation shows, the operation of the system is limited to purely ohmic fundamental mains behavior

$$\Phi = 0° \tag{49}$$

[cf., (41)]. The output voltage range is limited by the minimal value of the six-pulse diode bridge output voltage

$$U_{\mathrm{pn}} < \sqrt{\frac{3}{2}} U_{\mathrm{N,ll,rms}} \tag{50}$$

and therewith identical with the output voltage range for six-switch active buck-type PFC rectifier systems.

The PWM of S_+ and S_- can be implemented in phase or antiphase. The switching frequency ripple of i_{Y} is minimized for carrier signals $u_{\mathrm{D}+}$ and $u_{\mathrm{D}-}$ that are in phase. For carrier signals that are in opposite phase, a minimal output current ripple but a maximum ripple of i_{Y} results, which needs to be considered for the design of the filter capacitors C_{F} at the input.

A hardware demonstrator of the rectifier system is shown in Fig. 24. The transistors S_+ and S_- are implemented with latest generation of 1200-V high-speed IGBTs and the freewheeling diodes D_+ and D_- with SiC Schottky barrier diodes.

It should be noted that a hybrid third harmonic injection PFC rectifier circuit can also be built by combination of an active-filter-type third harmonic injection rectifier and a simple dc–dc buck converter stage as shown in Fig. 25. The buck stage to be controlled, e.g., for a constant output current or a constant output voltage then ensures, independent of the pulsation of the voltage $u_{\bar{\mathrm{p}}\bar{\mathrm{n}}}$ with sixfold mains frequency, a constant output power. The advantage of this circuit topology is that only a single power transistor is lying in the main current path, i.e., in particular, at high output voltages with a relatively short freewheeling interval, low conduction losses occur. In addition, the negative output voltage terminal is always connected to the mains via a diode of the lower bridge half of the diode rectifier. Therefore, no output CM voltage with switching frequency is generated. The implementation effort of the CM EMI filter can thus be reduced. Only the parasitic capacitors of the power semiconductors lead to high-frequency CM noise currents (cf., related consideration of boost-type PFC rectifier systems in [56]).

4) Discussion: The impression of the mains current of the considered buck-type PFC rectifier systems is obtained with so far known current control schemes always only in an indirect manner. This means that typically only the dc-link current but not the input currents is feedback-controlled to a load-dependent or predefined constant value. In these control schemes, block-shaped segments of the controlled dc-link current are injected by PWM of the rectifier input stage into the individual input lines such that after low-pass filtering with the input filter capacitors, sinusoidal currents are drawn from the mains. Accordingly, contrary to the boost-type PFC rectifiers (cf., Section IV-A5) with feedback-controlled input currents, concepts based on the current injection principle and direct active buck-type PFC rectifier systems typically use feed-forward control for the input currents and can, thus, be considered as equivalent regarding the achievable input current quality.

C. Systems With Boost-Type and Buck-Type Characteristic

As shown in Fig. 4, the output voltage range of boost-type PFC rectifiers is not immediately adjoining the output voltage range of buck-type systems. Voltages in the range

$$\sqrt{\frac{3}{2}} U_{\mathrm{N,ll,rms}} < U_{\mathrm{pn}} < \sqrt{2}\, U_{\mathrm{N,ll,rms}} \tag{51}$$

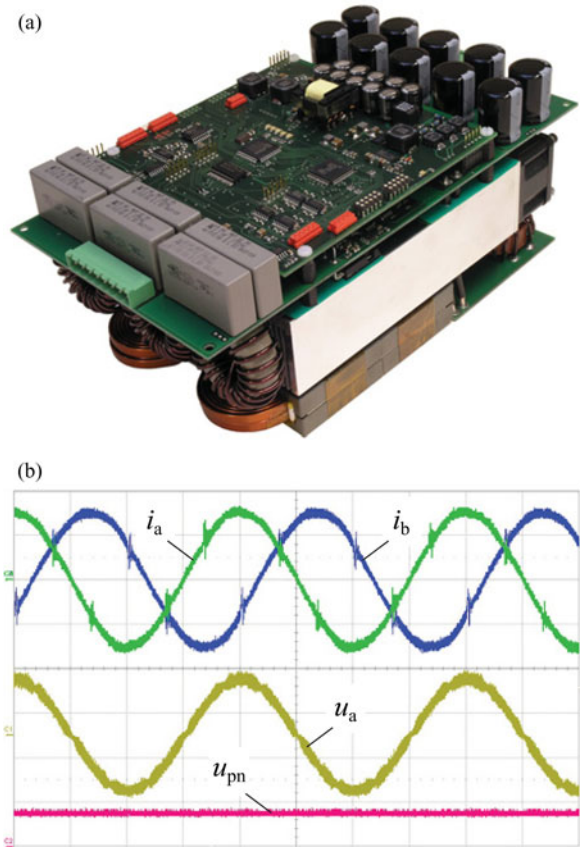

Fig. 24. (a) Hardware demonstrator of a 7.5-kW SWISS rectifier (dimensions: 210 mm × 132 mm × 92 mm; power density: $\rho = 2.94\,\mathrm{kW/dm^3} = 48\,\mathrm{W/in^3}$). (b) Time behavior of two phase currents, the input phase voltage, and the dc output voltage. Operating parameters: rms line-to-line input voltage $U_{\mathrm{N,ll,rms}} = 400\,\mathrm{V}$, mains frequency $f_{\mathrm{N}} = 50\,\mathrm{Hz}$, dc output voltage $U_{\mathrm{pn}} = 400\,\mathrm{V}$, and switching frequency $f_{\mathrm{P}} = 36\,\mathrm{kHz}$. The rectifier has a nominal efficiency of $\eta_{\mathrm{nom}} = 96.5\%$. Scales: 10 A/div, 250 V/div, 500 V/div, 5 ms/div (measurement performed with LC input filter not with EMI input filter).

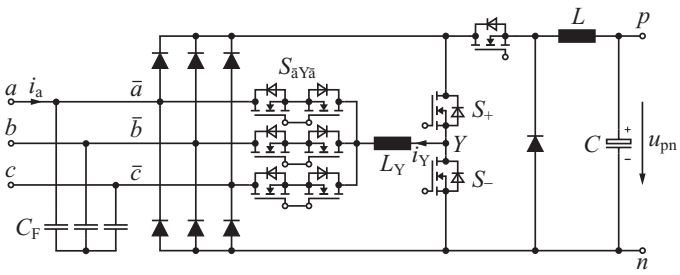

Fig. 25. Combination of an active-filter-type third harmonic current injection rectifier and a dc–dc buck-type converter stage to an active buck-type PFC rectifier system. The system is characterized by a minimal number of power semiconductors in the main current path, and only a low-frequency variation of the output CM voltage. The dc–dc buck converter should be advantageously implemented as interleaved converter.

can, thus, only be generated with a downstream dc–dc boost converter of the buck-type PFC rectifier or by combination of boost-type PFC rectifier and a dc–dc buck converter.

As an alternative to an explicit implementation of a dc–dc converter, a dc–dc boost converter stage could also be integrated into the output stage of a buck-type PFC system, whereby the output inductor could also be used as boost inductor [72], [73].

V. CONCLUSION

As shown in this first part of the paper, a three-phase PFC rectifier functionality can be implemented besides a phase-modular approach with 1) direct control of the conduction state of a three-phase rectifier through integrated power transistors or parallel control branches with active power semiconductors, i.e., as an active rectifier or 2) by shaping the output currents of a three-phase diode rectifier on the dc side and feedback/injection of the current difference always in that phase which would not conduct current for conventional passive diode rectification, i.e., as a hybrid rectifier with third harmonic current injection.

Following these basic concepts, direct three-phase rectifier circuits with boost- or buck-type characteristic are realizable. These circuits advantageously have a bridge topology (at the input) with bridge-legs of identical structure and, thus, feature an overall bridge symmetry.

For both circuit categories, over the last two decades, a variety of circuit topologies have been proposed. However, in the opinion of the authors, from the category of the boost-type rectifier systems, only the conventional (bidirectional) six-switch converter and the VIENNA rectifier and from the systems with buck-type characteristic only again the six-switch structure and the SWISS rectifier, proposed in this paper, are of interest for industrial application. Compared to these four topologies, other circuit concepts show a (significantly) higher complexity of the power and/or the control circuit, or have high-component stresses at a lower complexity and a limited operating range with regard to output voltage range and/or current-to-voltage phase displacement angle at the input. This is of particular importance when operating at unbalanced mains systems or in the case of failure of a mains phase.

The selected circuit topologies enable very high efficiencies as a result of the excellent conduction and switching characteristics of modern Si, SiC, and GaN power semiconductors. Soft-switching concepts are, thus, not necessary and would also not be accepted by industry due to the increase in complexity resulting from the auxiliary circuit branches with additional losses and due to the typically complex state sequence within a switching period. In general, in industry, only circuit topologies are practicable that are well understood not only by the inventors but also by a sufficiently large number of engineers.

In terms of system complexity, it should be noted that the restriction to unidirectional power flow does not allow a reduction, e.g., a halving of the number of active semiconductors or a simpler control scheme. The reason is that, ultimately, unidirectional structures also have to conduct phase currents of both directions and to generate voltages with both polarities. Only for three-level converters, a clear advantage of unidirectional converters (VIENNA rectifier) is given compared with bidirectional converters; for the unidirectional system, six transistors (with antiparallel diodes) and six diodes are required, whereas the implementation of a topologically similar bidirectional

T-type three-level converter system [74] requires twelve transistors (with antiparallel diodes).

The main three-phase PWM rectifier circuit topologies, except the SWISS rectifier, have been already theoretically investigated and experimentally verified in the literature. Therefore, for further academic research, mainly the following relatively narrow topics remain:

1) Direct mains (input) current control of buck-type PFC rectifier circuits. (For these systems, typically, only the output voltage and the output current is directly controlled and/or the mains current is not explicitly included in a feedback loop; thus, particularly for high mains frequencies (800 Hz), current distortions can occur at the intersections of the line-to-line voltages.)
2) Parallel operation of a higher number (more than two) converter systems. (High output power levels are often implemented by parallel connection of multiple low-power modules where circulating currents could occur in between the systems.)
3) Stability of distributed converter systems. (The constant power characteristic of PFC rectifiers results in a negative differential input impedance, which can lead to instability in combination with the EMI input filter or the inner mains impedance and/or with other converters [75].)

In addition to these topics, especially the multi-objective optimization of converter systems represents a wide and interesting field of research. When developing an industrial systems, besides a defined efficiency and power density, mainly a cost target has to be met, and a certain lifetime has to be guaranteed, i.e., multiple performance indices have to be simultaneously considered. It is, therefore, essential to understand the mutual dependence of the performance indices in the course of the design, e.g., the tradeoff between power density ρ (kW/dm^3) and efficiency η (%), which is shown in the second part of this paper [65] for four selected PFC rectifier systems.

ACKNOWLEDGMENT

The authors would like to thank Dr. M. Hartmann for providing figures and data of the VIENNA rectifier and the Δ-switch rectifier from his Ph.D. thesis [56].

REFERENCES

[1] P. Walther, "A new rectifier system high efficient, high dense, modular, quick to install and superior for service," in *Proc. 15th Int. Telecom. Energy Conf.*, Sep. 27–30, 1993, vol. 2, pp. 247–250.
[2] A. Pietkiewvicz and D. Tollik, "Cost/performance considerations for 1-phase input current shapers," in *Proc. 16th Int. Telecom. Energy Conf.*, Apr. 11–15, 1994, pp. 165–170.
[3] A. Kuperman, U. Levy, J. Goren, A. Zafranski, and A. Savernin, "High power Li-ion battery charger for electric vehicle," in *Proc. 7th Int. Compat. Power Electron. Conf.-Workshop*, Jun. 1–3, 2011, pp. 342–347.
[4] J. W. Kolar, T. Friedli, and M. Hartmann, "Three-phase PFC rectifier and ac–ac converter systems—Part I, Tutorial," in *Proc. 26th IEEE Appl. Power Electron. Conf. Expo.*, Mar. 6–10, 2011, pp. 1–268.
[5] D. A. Paice, *Power Electronics Converter Harmonics: Multipulse Methods for Clean Power*. Hoboken, NJ: Wiley, 1999.
[6] P. Pejovic, *Three-Phase Diode Rectifiers With Low Harmonics*. New York: Springer, 2007.
[7] T. Sakkos, V. Sarv, and J. Soojärv, "Optimum diode-switched active filters for power factor correction of single- and three-phase diode rectifiers with capactive smoothing," in *Proc. 7th Eur. Conf. Power Electron. Appl.*, Sep. 8–10, 1997, pp. 870–875.
[8] Y. Keping, D. Xiao, M. F. Rahman, and U. M. Nasir, "Applying reduced general direct space vector modulation approach of ac-ac matrix converter theory to achieve unity power factor controlled three-phase ac-dc matrix rectifier," in *Proc. 46th IEEE Ind. Appl. Soc. Annu. Meet.*, Oct. 9–13, 2011, pp. 1–7.
[9] K. Miyagawa, M. Nakaoka, Y. Ogino, Y. Murakami, and K. Hayashi, "Space-vector controlled soft-switching three-phase PDM ac/dc converter with unity power factor and sinusoidal line current," in *Proc. 18th IEEE Ind. Electron. Soc. Conf.*, Nov. 13–17, 1992, pp. 891–895.
[10] V. Vlatkovic, D. Borojevic, and F. C. Lee, "A zero-voltage switched, three-phase isolated PWM buck rectifier," *IEEE Trans. Power Electron.*, vol. 10, no. 2, pp. 148–157, Mar. 1995.
[11] J. W. Kolar and H. Ertl, "Status of the techniques of three-phase rectifier systems with low effects on the mains," in *Proc. 21st Int. Telecom. Energy Conf.*, Jun. 6–9, 1999, pp. 1–16.
[12] M. Rastogi, R. Naik, and N. Mohan, "Optimization of a novel dc-link current modulated interface with 3-phase utility systems to minimize line current harmonics," in *Proc. 23d IEEE Power Electron. Spec. Conf.*, Jun. 29–Jul. 3, 1992, pp. 162–167.
[13] R. Naik, M. Rastogi, N. Mohan, R. Nilssen, and C. P. Henze, "A magnetic device current injection in a three-phase sinusoidal-current utility interface," in *Proc. 28th IEEE Ind. Appl. Soc. Annu. Meet.*, Oct. 2–8, 1993, pp. 926–930.
[14] S. Kim, P. Enjeti, D. Rendusara, and I. J. Pitel, "A new method to improve THD and reduce harmonics generated by a three phase diode rectifier type utility interface," in *Proc. 29th IEEE Ind. Appl. Soc. Annu. Meet.*, Oct. 2–6, 1994, pp. 1071–1077.
[15] Y. Nishida, Y. Ohgoe, M. Nakaoka, and A. Maeda, "A simple three-phase boost-mode PFC rectifier," in *Proc. 31th IEEE Ind. Appl. Soc. Annu. Meet.*, Oct. 6–10, 1996, vol. 2, pp. 1056–1061.
[16] H. Yoo and S.-K. Sul, "A novel approach to reduce line harmonic current for a three-phase diode rectifier-fed electrolytic capacitor-less inverter," in *Proc. 24th IEEE Appl. Power Electron. Conf. Expo.*, Feb. 15–19, 2009, pp. 1897–1903.
[17] H. Yoo and S.-K. Sul, "A new circuit design and control to reduce input harmonic current for a three-phase ac machine drive system having a very small dc-link capacitor," in *Proc. 25th IEEE Appl. Power Electron. Conf. Expo.*, Feb. 21–25, 2010, pp. 611–618.
[18] H. Ertl and J. W. Kolar, "A constant output current three-phase diode bridge rectifier employing a novel electronic smoothing inductor," *IEEE Trans. Ind. Electron.*, vol. 52, no. 2, pp. 454–461, Apr. 2005.
[19] K. Mino, M. L. Heldwein, and J. W. Kolar, "Ultra compact three-phase rectifier with electronic smoothing inductor," in *Proc. 20th IEEE Appl. Power Electron. Conf. Expo.*, Mar. 6–8, 2005, vol. 1, pp. 522–528.
[20] T. Takaku, G. Homma, T. Isober, S. Igarashi, Y. Uchida, and R. Shimada, "Improved wind power conversion system using magnetic energy recovery switch (MERS)," in *Proc. 40th IEEE Ind. Appl. Soc. Annu. Meet.*, Oct. 2–6, 2005, vol. 3, pp. 2007–2012.
[21] J. A. Wiik, F. D. Widjaya, T. Isobe, T. Kitahara, and R. Shimada, "Series connected power flow control using magnetic energy recovery switch (MERS)," in *Proc. IEEE/IEEJ Power Convers. Conf.*, Apr. 2–5, 2007, pp. 983–990.
[22] K. D. Ngo, "Topology and analysis in PWM inversion, rectification, and cyclconversion," Ph.D. dissertation, Electr. Eng. Dept., California Inst. Technol., Pasadena, 1984.
[23] J. W. Kolar, H. Sree, U. Drofenik, N. Mohan, and F. C. Zach, "A novel three-phase three-switch three-level high power factor SEPIC-type ac-to-dc converter," in *Proc. 12th IEEE Appl. Power Electron. Conf. Expo.*, Feb. 23–27, 1997, vol. 2, pp. 657–665.
[24] L. Huber, L. Gang, and M. M. Jovanovic, "Design-oriented analysis and performance evaluation of buck PFC front-end," in *Proc. 24th IEEE Appl. Power Electron. Conf. Expo.*, Feb. 15–19, 2009, pp. 1170–1176.
[25] J. W. Kolar, U. Drofenik, and F. C. Zach, "VIENNA Rectifier II—A novel single-stage high-frequency isolated three-phase PWM rectifier system," in *Proc. 13th IEEE Appl. Power Electron. Conf. Expo.*, Feb. 15–19, 1998, vol. 1, pp. 23–33.
[26] D. S. Greff and I. Barbi, "A single-stage high-frequency isolated three-phase ac/dc converter," in *Proc. 32nd IEEE Ind. Electron. Soc. Conf.*, Nov. 6–10, 2006, pp. 2648–2653.
[27] J. Miniboeck, R. Greul, and J. W. Kolar, "Evaluation of a delta-connection of three single-phase unity power factor rectifier modules (Δ-rectifier) in

comparison to a direct three-phase rectifier realization," in *Proc. 23rd Int. Telecom. Energy Conf.*, Oct. 14–18, 2001, pp. 446–454.

[28] R. Greul, S. D. Round, and J. W. Kolar, "Analysis and control of a three-phase, unity power factor Y-Rectifier," *IEEE Trans. Power Electron.*, vol. 22, no. 5, pp. 1900–1911, Sep. 2007.

[29] R. Greul, "Modulare Dreiphasen Pulsgleichrichtersysteme," Ph.D. dissertation, no. 16370, Power Electron. Sys. Lab., ETH Zurich, Zurich, Switzerland, 2005.

[30] J. W. Kolar, "Vorrichtung zur regelung der phasenzwischenkreisspannungen einer sternschaltung einphasiger pulsgleichrichtersysteme in analogie zu dreiphasen-dreipunkt-pulsgleichrichtersystemen," Swiss Patent CH699 822, 2010.

[31] J. Biela, U. Drofenik, F. Krenn, J. Minibock, and J. W. Kolar, "Novel three-phase Y-rectifier cyclic 2-out-of-3 dc output voltage balancing," in *Proc. 29th Int. Telecom. Energy Conf.*, Sep. 30–Oct. 4, 2007, pp. 677–685.

[32] J. W. Kolar, J. Biela, and J. Minibock, "Exploring the Pareto front of multi-objective single-phase PFC rectifier design optimization—99.2% efficiency vs. $7\,\mathrm{kW/dm^3}$ power density," in *Proc. 6th IEEE Int. Power Electron. Motion Control Conf.*, May. 17–20, 2009, pp. 1–21.

[33] D. Chapman, D. James, and C. J. Tuck, "A high density 48 V200 A rectifier with power factor correction—An engineering overview," in *Proc. 15th Int. Telecom. Energy Conf.*, Sep. 27–30, 1993, vol. 1, pp. 118–125.

[34] M. Karlsson, C. Thoren, and T. Wolpert, "A novel approach to the design of three-phase ac/dc power converters with unity power factor," in *Proc. 21st Int. Telecom. Energy Conf.*, Jun. 6–9, 1999, pp. 5–7.

[35] M. Karlsson, C. Thoren, and T. Wolpert, "Practical considerations concerning a novel 6 kW three-phase ac/dc power converter with unity power factor," in *Proc. 22nd Int. Telecom. Energy Conf.*, Sep. 10–14, 2000, pp. 28–33.

[36] R. Ridley, S. Kern, and B. Fuld, "Analysis and design of a wide input range power factor correction circuit for three-phase applications," in *Proc. 8th IEEE Appl. Power Electron. Conf. Expo.*, Mar. 7–11, 1993, pp. 299–305.

[37] J. W. Kolar, U. Drofenik, J. Miniböck, and H. Ertl, "A new concept for minimizing high-frequency common-mode EMI of three-phase PWM rectifier systems keeping high utilization of the output voltage," in *Proc. 15th IEEE Appl. Power Electron. Conf. Expo.*, Feb. 6–10, 2000, vol. 1, pp. 519–527.

[38] R. Grinberg, F. Canales, and M. Paakkinen, "Comparison study of full-bridge and reduced switch count three-phase voltage source inverters," in *Proc. 7th Int. Compat. Power Electron. Conf.-Workshop*, Jun. 1–3, 2011, pp. 270–275.

[39] *CoolMOS C3* 900 *V—First 900V High Voltage Power MOSFET Using Charge Compensation Principle*, Infineon, Neubiberg, Germany, 2008.

[40] B. Weis, M. Braun, and P. Friedrichs, "Turn-off and short circuit behaviour of 4H SiC JFETs," in *Proc. 36th IEEE Ind. Appl. Soc. Annu. Meet.*, Sep. 30–Oct. 4, 2001, vol. 1, pp. 365–369.

[41] T. Friedli, S. D. Round, and J. W. Kolar, "A 100 kHz SiC Sparse Matrix Converter," in *Proc. 38th IEEE Power Electron. Spec. Conf.*, Jun. 17–21, 2007, pp. 2148–2154.

[42] D. Aggeler, J. Biela, and J. W. Kolar, "Controllable du/dt behaviour of the SiC MOSFET/JFET cascode—An alternative hard commutated switch for telecom applications," in *Proc. 25th IEEE Appl. Power Electron. Conf. Expo.*, Feb. 21–25, 2010, pp. 1584–1590.

[43] B. Hull, M. Das, F. Husna, R. Callanan, A. Agarwal, and J. Palmour, "20 A, 1200 V 4H-SiC DMOSFETs for energy conversion systems," in *Proc. 1st IEEE Energy Convers. Congr. Expo.*, Sep. 20–24, 2009, pp. 112–119.

[44] J. W. Kolar, H. Ertl, and F. C. Zach, "Space vector-based analytical analysis of the input current distortion of a three-phase discontinuous-mode boost rectifier system," in *Proc. 24th IEEE Power Electron. Spec. Conf.*, Jun. 20–24, 1993, pp. 696–703.

[45] J. Sun and H. Grotstollen, "Averaged modeling and analysis of resonant converters," in *Proc. 24th IEEE Power Electron. Spec. Conf.*, Jun. 20–24, 1993, pp. 707–713.

[46] Q. Huang and F. C. Lee, "Harmonic reduction in a single-switch, three-phase boost rectifier with high order harmonic injected PWM," in *Proc. 27th IEEE Power Electron. Spec. Conf.*, Jun. 23–27, 1996, vol. 2, pp. 1266–1271.

[47] D. J. Perreault and J. G. Kassakian, "Design and evaluation of a cellular rectifier system with distributed control," in *Proc. 29th IEEE Power Electron. Spec. Conf.*, May 17–22, 1998, vol. 1, pp. 790–797.

[48] P. Barbosa, F. Canales, J.-C. Crebier, and F. C. Lee, "Interleaved three-phase boost rectifiers operated in the discontinuous conduction mode: Analysis, design considerations and experimentation," *IEEE Trans. Power Electron.*, vol. 16, no. 5, pp. 724–734, Sep. 2001.

[49] J. C. Salmon, "Comparative evaluation of circuit topologies for 1-phase and 3-phase boost rectifiers operated with a low current distortion," in *Proc. Canadian Conf. Electr. Comput. Eng.*, Sep. 25–28, 1994, pp. 30–33.

[50] R. Naik, M. Rastogi, and N. Mohan, "Third-harmonic modulated power electronics interface with 3-phase utility to provide a regulated dc output and to minimize line-current harmonics," in *Proc. 27th IEEE Ind. Appl. Soc. Annu. Meet.*, 1992, pp. 689–694.

[51] J. C. Salmon, "Operating a three-phase diode rectifier with a low-input current distortion using a series-connected dual boost converter," *IEEE Trans. Power Electron.*, vol. 11, no. 4, pp. 592–603, Jul. 1996.

[52] S. Kim, P. Enjeti, P. Packebush, and I. Pitel, "A new approach to improve power factor and reduce harmonics in a three phase diode rectifier type utility interface," in *Proc. 28th IEEE Ind. Appl. Soc. Annu. Meet.*, Oct. 2–8, 1993, pp. 993–1000.

[53] M. Jantsch and C. W. G. Verhoeve, "Inverters with three-phase output and without electrolyte capacitor for improved lifetime, efficiency and costs of grid connected systems," in *Proc. 14th Eur. Photovolt. Sol. Energy Conf. Exhib.*, Jun. 30–Jul. 4, 1997, pp. 1–3.

[54] J. W. Kolar, J. Ertl, and F. C. Zach, "Realization consideration for unidirectional three-phase PWM rectifier systems with low effects on the mains," in *Proc. 6th Europ. Power Electron. Motion Control Conf.*, Oct. 1–3, 1990, vol. 2, pp. 560–565.

[55] M. Hartmann, J. Miniböck, and J. W. Kolar, "A three-phase delta switch rectifier for more electric aircraft applications employing a novel PWM current control concept," in *Proc. 24th IEEE Appl. Power Electron. Conf. Expo.*, Feb. 15–19, 2009, pp. 1633–1640.

[56] M. Hartmann, "Ultra-compact and ultra-efficient three-phase PWM rectifier systems for more electric aircraft," Ph.D. dissertation, no. 19755, Power Electron. Sys. Lab., ETH Zurich, Zurich, Switzerland, 2011.

[57] J. W. Kolar and F. C. Zach, "A novel three-phase three-switch three-level PWM rectifier," in *Proc. 28th Power Convers. Conf.*, Jun. 28–30, 1994, pp. 125–138.

[58] Y. Zhao, Y. Li, and T. A. Lipo, "Force commutated three level boost type rectifier," in *Proc. 28th IEEE Ind. Appl. Soc. Annu. Meet.*, Oct. 2–8, 1993, pp. 771–777.

[59] M. L. Heldwein, S. A. Mussa, and I. Barbi, "Three-phase multilevel PWM rectifiers based on conventional bidirectional converters," *IEEE Trans. Power Electron.*, vol. 25, no. 3, pp. 545–549, Mar. 2010.

[60] F. Stögerer, J. Minibock and J. W. Kolar, "Implementation of a novel control concept for reliable operation of a VIENNA Rectifier under heavily unbalanced mains voltage conditions," in *Proc. 34nd IEEE Power Electron. Spec. Conf.*, Jun. 17–21, 2001, vol. 3, pp. 1333–1338.

[61] J. Miniböck, F. Stögerer and J. W. Kolar, "A novel concept for mains voltage proportional input current shaping of a VIENNA Rectifier eliminating controller multipliers, Part I—Basic theoretical considerations and experimental verification," in *Proc. 16th IEEE Appl. Power Electron. Conf. Expo.*, Mar. 4–8, 2001, vol. 1, pp. 582–586.

[62] F. Stögerer, J. Miniböck and J. W. Kolar, "A novel concept for mains voltage proportional input current shaping of a VIENNA Rectifier eliminating controller multipliers, Part II—Operation for heavily unbalanced mains phase voltages and in wide input voltage range," in *Proc. 16th IEEE Appl. Power Electron. Conf. Expo.*, Mar. 4–8, 2001, vol. 1, pp. 587–591.

[63] J. W. Kolar, U. Drofenik, and F. C. Zach, "Current handling capability of the neutral point of a three-phase/switch/level boost-type PWM (VIENNA) Rectifier," in *Proc. 27th IEEE Power Electron. Spec. Conf.*, Jun. 23–27, 1996, vol. 2, pp. 1329–1336.

[64] D. Krähenbühl, C. Zwyssig, K. Bitterli, M. Imhof, and J. W. Kolar, "Evaluation of ultra-compact rectifiers for low power, high-speed, permanent-magnet generators," in *Proc. 35th IEEE Ind. Electron. Soc. Conf.*, Nov. 3–5, 2009, pp. 448–455.

[65] T. Friedli, M. Hartmann, and J. W. Kolar, "The essence of three-phase PFC rectifier systems—Part II," *IEEE Trans. Power Electron.*, in publication, 2012.

[66] K. P. Phillips, "Current-source converter for ac motor drives," *IEEE Trans. Ind. Appl.*, vol. IA-8, no. 6, pp. 679–683, Nov. 1972.

[67] F. Schafmeister, "Indirekte Sparse Matrix Konverter," Ph.D. dissertation, no. 17428, Power Electron. Sys. Lab., ETH Zurich, Zurich, Switzerland, 2007.

[68] J. W. Kolar, T. Friedli, and M. Hartmann, "Three-phase PFC rectifier and ac-ac converter systems—Part II, Tutorial," in *Proc. 26th IEEE Appl. Power Electron. Conf. Expo.*, Mar. 6–10, 2011.

[69] T. C. Green, M. H. Taha, N. A. Rahim, and B. W. Williams, "Three-phase step-down reversible ac-dc power converter," *IEEE Trans. Power Electron.*, vol. 12, no. 2, pp. 319–324, Mar. 1997.

[70] A. Stupar, T. Friedli, J. Miniboeck, M. Schweizer, and J. W. Kolar, "Towards a 99% efficient three-phase buck-type PFC rectifier for 400 V dc distribution systems," in *Proc. 26th IEEE Appl. Power Electron. Conf. Expo.*, Mar. 6–10, 2011, pp. 505–512.
[71] M. Hartmann, T. Friedli, and J. W. Kolar, "Three-phase unity power factor mains interfaces of high power EV battery charging systems," in *Proc. Power Electron. Charging Electric Veh. Workshop*, Mar. 21–22, 2011.
[72] J. W. Kolar, "Netzrückwirkungsarmes Dreiphasen-Stromzwischenkreis-Pulsgleichrichtersystem mit weitem Stellbereich der Ausgangsspannung," Worldwide Patent WO 01/50 583 A1, 2001.
[73] T. Nussbaumer, K. Mino, and J. W. Kolar, "Design and comparative evaluation of three-phase buck-boost and boost-buck unity power factor PWM rectifier systems for supplying variable dc voltage link converters," in *Proc. 10th Eur. Power Quality Conf.*, May. 25–27, 2004, pp. 126–135.
[74] M. Schweizer, I. Lizama, T. Friedli, and J. W. Kolar, "Comparison of the chip area usage of 2-level and 3-level voltage source converter topologies," in *Proc. 36th IEEE Ind. Electron. Soc. Conf.*, Nov. 7–11, 2010, pp. 391–396.
[75] M. Schweizer and J. W. Kolar, "Shifting input filter resonances—An intelligent converter behavior for maintaining system stability," in *Proc. IEEE/IEEJ Int. Power Electron. Conf.*, Jun. 21–24, 2010, pp. 906–913.

Johann W. Kolar (F'10) received the M.Sc. and Ph.D. degrees (*summa cum laude*/*promotio sub auspiciis praesidentis rei publicae*) from the Vienna University of Technology Vienna, Austria, in 1997 and 1998, respectively.

Since 1984, he has been working as an independent international Consultant in close collaboration with the Vienna University of Technology, in the fields of power electronics, industrial electronics, and high-performance drives. He has proposed numerous novel converter topologies and modulation/control concepts, e.g., the VIENNA rectifier, the SWISS rectifier, and the three-phase ac–ac sparse matrix converter. He has published more than 450 scientific papers in international journals and conference proceedings and has filed more than 85 patents. He joined as Professor and Head of the Power Electronic Systems Laboratory, Swiss Federal Institute of Technology, Zurich, Switzerland, on Feb. 1, 2001. He initiated and/or is the founder/cofounder of four spin-off companies targeting ultra-high speed drives, multidomain/level simulation, ultra-compact/efficient converter systems and pulsed power/electronic energy processing. His current research focuses on ac–ac and ac–dc converter topologies with low effects on the mains, e.g., for data centers, more-electric-aircraft and distributed renewable energy systems, and on solid-state transformers for smart microgrid systems. Further research areas include the realization of ultra-compact and ultra-efficient converter modules employing latest power semiconductor technology (SiC and GaN), micropower electronics and/or power supplies on chip, multidomain/scale modeling/simulation and multi-objective optimization, physical model-based lifetime prediction, pulsed power, and ultra-high-speed and bearingless motors.

Dr. Kolar received the Best Transactions Paper Award of the IEEE Industrial Electronics Society (IES) in 2005, the Best Paper Award of the International Conference on Power Electronics in 2007, the 1st Prize Paper Award of the IEEE Industry Applications Society (IAS) Industrial Power Converters Committee in 2008, the IEEE IECON Best Paper Award of the IES Power Electronics Technical Committee in 2009, the IEEE Power Electronics Society (PELS) Transaction Prize Paper Award in 2009, the Best Paper Award of the IEEE/ASME TRANSACTIONS ON MECHATRONICS in 2010, the IEEE PELS Transactions Prize Paper Award in 2010, the Best Paper 1st Prize Award at the ECCE Asia 2011, and the 1st Place IEEE IAS Prize Paper Award in 2011. He became an IEEE Distinguished Lecturer of the IEEE PELS in 2011. Furthermore, he received the ETH Zurich Golden Owl Award in 2011 for excellent teaching. He is a member of the Institution of Electrical Engineers of Japan (IEEJ) and of International Steering Committees and Technical Program Committees of numerous international conferences in the field (e.g., Director of the Power Quality Branch of the International Conference on Power Conversion and Intelligent Motion). He is the founding Chairman of the IEEE PELS Austria and Switzerland Chapter and Chairman of the Education Chapter of the European Power Electronics and Drives Association. From 1997 to 2000, he was an Associate Editor of the IEEE TRANSACTIONS ON INDUSTRIAL ELECTRONICS and since 2001 he has been an Associate Editor of the IEEE TRANSACTIONS ON POWER ELECTRONICS. Since 2002, he has also been an Associate Editor of the *Journal of Power Electronics* of the Korean Institute of Power Electronics and a member of the Editorial Advisory Board of the IEEJ Transactions on Electrical and Electronic Engineering.

Thomas Friedli (M'09) received the M.Sc. degree in electrical engineering and information technology (with distinction) and the Ph.D. degree from the Swiss Federal Institute of Technology (ETH Zurich), Zurich, Switzerland, in 2005 and 2010, respectively.

From 2006 to 2011, he was with the Power Electronic Systems Laboratory, ETH Zurich, where he performed research on current source and matrix converter topologies using silicon carbide power semiconductors, active three-phase PFC rectifiers, and conducted electromagnetic interference. Since 2012, he has been with ABB Switzerland Ltd., Turgi, Switzerland, as an R&D Engineer for power electronics and medium voltage drives for traction converter systems. His current research interests include the areas of high-efficiency power electronic systems and their control, three-phase power converters, electromagnetic interference, and applications of wide bandgap power devices.

Dr. Friedli received the 1st Prize Paper Award of the IEEE Industrial Applications Society Industrial Power Converters Committee in 2008 and the IEEE TRANSACTIONS ON INDUSTRY APPLICATIONS Prize Paper Award in 2009.